International Geology Review

ISSN: 0020-6814 (Print) 1938-2839 (Online) Journal homepage: http://www.tandfonline.com/loi/tigr20

Petrogenesis of Early Cretaceous low-Mg adakitic rocks along the southernmost margin of the North China Craton: implications for late Mesozoic crustal evolution

Longyao Chen, Wei Qu & Shuwen Liu

INTERNATIONAL GEOLOGY REVIEW, 2017
VOL. 59, NO. 8, 996–1014
http://dx.doi.org/10.1080/00206814.2016.1242094

Taylor & Francis
Taylor & Francis Group

Check for updates

Petrogenesis of Early Cretaceous low-Mg adakitic rocks along the southernmost margin of the North China Craton: implications for late Mesozoic crustal evolution

Longyao Chen[a,b], Wei Qu[a] and Shuwen Liu[b]

[a]Institute of Geomechanics, Chinese Academy of Geological Sciences, Beijing, PR China; [b]School of Earth and Space Sciences, Peking University, Beijing, PR China

ABSTRACT

This article reports systematic zircon U–Pb dating, whole-rock geochemistry, and Sr–Nd isotopic data for the Early Cretaceous Jialou granitoids along the southernmost margin of the North China Craton (NCC), adjacent to the Tongbai Orogen. These results will provide significant constrains on the crustal evolution of the southern margin of the NCC. Zircon U–Pb analyses, using laser ablation–multicollector–inductively coupled plasma–mass spectrometry, indicate that the Jialou granitoids were emplaced at ~130 Ma. The granitoids have high SiO_2, K_2O, Al_2O_3, Sr, and Ba contents, high Sr/Y and (La/Yb)N ratios, and low concentrations of MgO, Y, and heavy rare earth elements, indicating a low-Mg adakitic affinity. They have relatively high initial $^{87}Sr/^{86}Sr$ ratios (0.707464–0.708190) and negative εNd(t) values (−11.8 to −15.2), similar to those of the Palaeoproterozoic lower crust in the NCC. These geochemical and isotopic features indicate that the Jialou low-Mg adakitic rocks were derived by partial melting of mafic Palaeoproterozoic lower crust of the NCC at >50 km depth, leaving behind a garnet amphibolite residue. The petrogenesis of the Jialou low-Mg adakitic rocks, plus the petrogenesis of Mesozoic granitoids and lower crustal xenoliths entrained in the Late Jurassic Xinyang volcaniclastic diatreme, suggests that the continental crust along the southern margin of the NCC was thickened during the Middle Jurassic to Early Cretaceous, but thinned after 130 Ma. We propose that crustal thickening was caused by a late Middle Jurassic to Early Cretaceous intra-continental orogeny, rather than continent–continent collision between the NCC and the Yangtze Craton. We also suggest that crustal thinning and Early Cretaceous magmatism were related to subduction of the palaeo-Pacific plate, rather than post-orogenic collapse of the Qinling–Tongbai–Dabie Orogen.

ARTICLE HISTORY
Received 5 July 2016
Accepted 25 September 2016

KEYWORDS
Low-Mg adakitic rocks; petrogenesis; crustal evolution; North China Craton

1. Introduction

It is generally accepted that the North China Craton (NCC) has experienced significant lithospheric thinning and decratonization since the Mesozoic. The contrasting compositions of mantle xenoliths in Palaeozoic diamondiferous kimberlites and those in Cenozoic basalts suggests that >100 km of the ancient lithosphere was removed during the late Mesozoic and Cenozoic (Fan and Menzies 1992; Menzies *et al*. 1993, 2007; Zheng *et al*. 1998; Fan *et al*. 2000; Gao *et al*. 2002; Rudnick *et al*. 2004). Comprehensive geological studies of the NCC, involving the analysis of petrological, geochemical, geochronological, and geophysical data, have been used to elucidate the timing and mechanism of lithospheric thinning (Menzies *et al*. 1993; 2007; Zheng *et al*. 1998; Gao *et al*. 2002; 2004; Wu *et al*. 2005; and references therein). Two prevailing models have been proposed for the thinning process of the NCC lithosphere: (1) thermo-chemical erosion (Menzies *et al*. 1993; 2007; Y.G. Xu 2001; Y.G. Xu *et al*. 2004; Zheng *et al*. 1998), and (2) delamination (Gao *et al*. 2002; 2004; W.L. Xu *et al*. 2006; 2008; Wu *et al*. 2005). However, crustal evolution corresponding to lithospheric thinning specifically during the Mesozoic has been poorly studied.

The formation sequence of various types of magmatism is generally used to constrain the tectonic and crustal evolution of a region. Mesozoic granitoids are widespread along the southern margin of the NCC (Mao *et al*. 2010; Wang *et al*. 2011, 2013). Zircon U–Pb dating shows that the Mesozoic granitoid magmatism may be divided into three episodes: (1) Late Triassic (225–200 Ma), (2) Late Jurassic to Early Cretaceous (160–130 Ma), and (3) Early Cretaceous (130–110 Ma). The

CONTACT Longyao Chen chenlongyao1220@163.com Institute of Geomechanics, Chinese Academy of Geological Sciences, 11 Minzudaxue Nanlu, Beijing 100081, P. R. China
Supplemental data for this article can be accessed here.

granitoids provide a valuable opportunity to understand the crustal evolution of the southern margin of the NCC during the Mesozoic. In addition, a number of granitoid-hosted gold and molybdenum deposits occurred along the western side of the southern margin of the NCC, adjacent to the Qinling Orogen (Chen *et al*. 1998, 2007; Mao *et al*. 2002, 2005, 2011; Chen 2006; Deng *et al*. 2016; Hu *et al*. 2016). Therefore, the majority of previous investigations on the Mesozoic granitoids in the southern margin of the NCC were focused on the western segment (the Xiaoqinling and Xiong'ershan areas) (Guo *et al*. 2009; Gao *et al*. 2010, 2014a, 2014b; Ding *et al*. 2011; Qi *et al*. 2012; Wang *et al*. 2011, 2013; Hu *et al*. 2012; Zhao *et al*. 2012a), and only a few studies are focused on the eastern segment Mesozoic granitoids in the Jialou area, where is adjacent to the Tongbai Orogen (Zhao *et al*. 2008). However, the origin and geodynamic background of the Mesozoic granitoids still remain unclear in the eastern segment, which have affected the better understanding of crustal evolution of the southern margin of the NCC.

In this article, we report geochronological, geochemical, and Sr–Nd isotopic data for the Jialou pluton at the southernmost margin of the NCC, in order to investigate its petrogenesis and magma source of the granitoids. The crustal evolution of the southern margin of the NCC will be discussed, taking into consideration the results of previous research conducted on the Mesozoic granitoids in the area.

2. Geological setting

The NCC is bordered by the late Palaeozoic Central Asian orogenic belt to the north, the early Palaeozoic Kunlun–Qilian Orogen to the west, the Mesozoic Qinling–Tongbai–Dabie Orogen to the south, and the Su–Lu ultrahigh-pressure metamorphic belt to the east (Figure 1(a)). The southern margin of the NCC is bounded by the Lingbao–Wuyang Fault to the north, and is separated from the Qinling–Tongbai–Dabie Orogen by the Luonan–Luanchuan Fault in the south (Figure 1(b)).

The southern margin of the NCC was involved into the Mesozoic–Cenozoic intra-continental orogenic deformation (Zhang *et al*. 2001; Xu *et al*. 2009). The region has the consistent basement-cover sequence with the inner NCC. The basement is dominated by 2.8–2.5 Ga tonalitic–trondhjemitic–granodioritic (TTG) gneisses and Archean to Palaeoproterozoic supracrustal rocks of the Taihua Group, comprising mainly amphibolite, felsic gneiss, migmatite, quartzite, and marbles (Kröner *et al*. 1988; Wan *et al*. 2006; Xu *et al*. 2009). The extensively exposed Palaeoproterozoic volcanic rocks of the Xiong'er Group (1.75–1.78 Ga) unconformably overlie Archean to Palaeoproterozoic basement rocks and consist predominantly of intermediate–acidic lavas and pyroclastic rocks interlayered with minor sedimentary rocks (Zhao *et al*. 2004, 2009). The Xiong'er volcanic rocks are unconformably overlain by Meso- to Neoproterozoic terrigenous sandstones, limestones, and

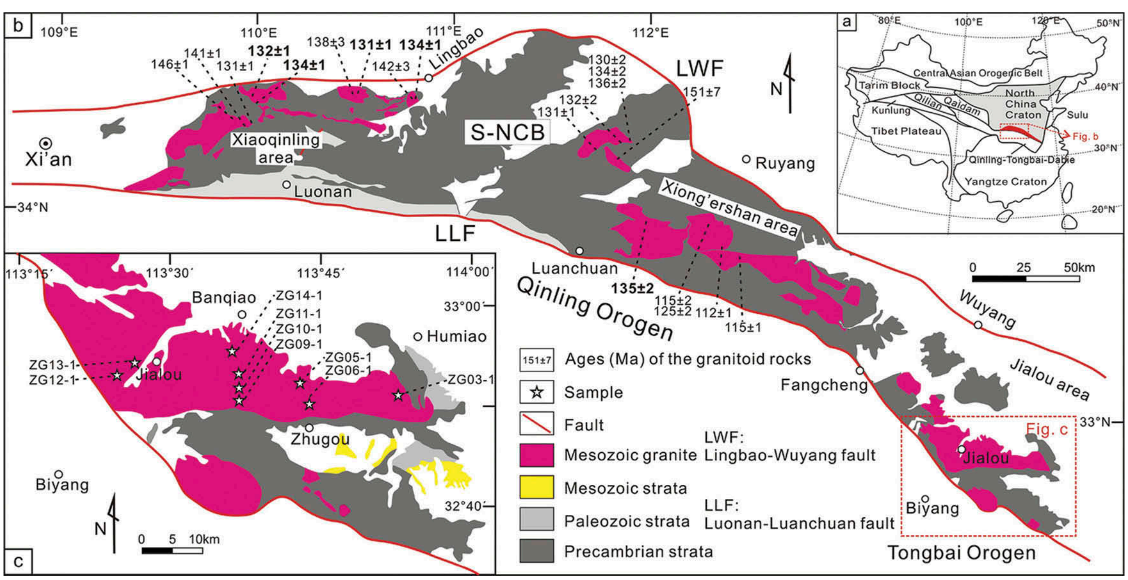

Figure 1. (a) Simplified geological map of China showing the major tectonic blocks surrounding the North China Craton (NCC) and the location of the southern margin of the NCC (red lines). (b) Geological map of the southern margin of the NCC showing distribution of the Late Mesozoic granitoids (modified from Dong *et al*. 2015). The fold fonts such as **134 ± 1** represent the ages (Ma) of the granitoids with adakitic affinity. Major rock sampling locations are listed in Table 1. Age data sources: Xiaoqinling area (Zhu *et al*. 2008; Guo *et al*. 2009; Mao *et al*. 2010; Hu *et al*. 2012; Zhao *et al*. 2012a), Xiong'ershan area (Guo *et al*. 2009; Mao *et al*. 2010; Gao *et al*. 2014a, 2014b). (c) Geological map of the Jialou granitoids. The sampling localities of the studied rocks are indicated.

calcsilicate rocks of Guandaokou Group and the Luanchuan Group (Lu *et al.* 2008; Hu *et al.* 2014). These rocks are locally overlain by a Sinian to Ordovician passive continental margin sequence composing chiefly of platform carbonates, shales, and sandstones (Xue *et al.* 1996; Zhang *et al.* 2001). The Xiaoqinling, Xiong'ershan, and Jialou areas are uplifted basement terranes, scattering along the southern margin of the NCC from west to east (Figure 1(b)). These basement terranes were uplifted during the Jurassic to Cretaceous because of intracontinental extension and emplacement of granitic magma (Liu *et al.* 1998; Zhang and Zheng 1999).

Multiple stages of magmatic activity are recognized along the southern margin of the NCC, as inferred from the presence of Neoarchean tonalite–trondhjemite–granodiorite (TTG) rocks, Palaeo-Mesoproterozoic granites, and voluminous Mesozoic granitoids. The Mesozoic magmatism may be divided into three episodes: Late Triassic, Late Jurassic to Early Cretaceous, and Early Cretaceous (Table 1). The Late Triassic granitoids only occur in the Xiaoqinling area and consist chiefly of biotite monzogranites, quartz diorites, quartz monzonites, and hornblende monzonites (Ding *et al.* 2011; Qi *et al.* 2012). Most previous studies suggested that these granitoids formed in a post-collisional extensional

Table 1. Summary of sample localities, lithology, and ages of the late Mesozoic granitoids in the southern margin of the NCC. The granitoids marked by '*' have low-Mg adakitic affinity.

Sample	Location	Coordinates	Lithology	Age(Ma)	Method	Reference
Xiaoqinling area						
M0601	Laoniushan	N 34°20′15.8″ E 109°57′48.3″	Monzogranite	146 ± 1	Zircon U-Pb LA-ICPMS	Zhu *et al.* (2008)
JD01	Jinduicheng	N 34°19′48.5″ E 109°57′16.3″	Granite porphyry	141 ± 1	Zircon U-Pb LA-ICPMS	Zhu *et al.* (2008)
LF04*	Huashan	N 34°28′01.7″ E 109°57′51.7″	Monzogranite	134 ± 1	Zircon U-Pb LA-ICPMS	Guo *et al.* (2009)
ZB2	Huanglongpu	N 34°21′18″ E 110°01′52.8″	Monzogranite	131 ± 1	Zircon U-Pb SHRIMP	Mao *et al.* (2010)
NN1	Niangniangshan	N 34°26′29″ E 110°47′46″	Monzogranite	142 ± 3	Zircon U-Pb LA-ICPMS	Mao *et al.* (2010)
YWS3	Wenyu	N 34°39′36″ E 110°24′44″	Monzogranite	138 ± 3	Zircon U-Pb LA-ICPMS	Mao *et al.* (2010)
HS10*	Fangshanyu	N 34°28′26.1″ E 109°57′51.8″	Monzogranite	132 ± 1	Zircon U-Pb LA-ICPMS	Hu *et al.* (2012)
W-4*	Wenyu		Monzogranite	131 ± 1	Zircon U-Pb LA-ICPMS	Zhao *et al.* (2012a)
N-3*	Niangniangshan		Monzogranite	134 ± 1	Zircon U-Pb LA-ICPMS	Zhao *et al.* (2012a)
Xiong'ershan area						
HP2	Haoping	N 34°16′46″ E 109°41′34″	Granite	131 ± 1	Zircon U-Pb SHRIMP	Mao *et al.* (2010)
HS2	Huashan	N 34°19′17″ E 109°49′42″	Monzogranite	132 ± 2	Zircon U-Pb SHRIMP	Mao *et al.* (2010)
HY02*	Heyu	N 34°59′32.4″ E 111°51′45″	Monzogranite	135 ± 2	Zircon U-Pb LA-ICPMS	Guo *et al.* (2009)
LM2	Leimengou	N 34°11′42″ E 111°31′37″	Granite porphyry	136 ± 2	Zircon U-Pb SHRIMP	Mao *et al.* (2010)
WZS1	Wuzhuangshan	N 34°09′05″ E 111°59′38″	Monzogranite	157 ± 1	Zircon U-Pb SHRIMP	Mao *et al.* (2010)
MG	Mogou	N 34°06′13″ E 112°04′03″	Granite porphyry	134 ± 2	Zircon U-Pb SHRIMP	Mao *et al.* (2010)
HPGB10	Haopinggou	N 34°10′48″ E 112°04′03″	Granite porphyry	130 ± 2	Zircon U-Pb SHRIMP	Mao *et al.* (2010)
DG-B5	Donggou	N 33°57′00″ E 112°22′48″	Granite porphyry	112 ± 1	Zircon U-Pb SHRIMP	Mao *et al.* (2010)
TSM5	Taishanmiao	N 33°49′07″ E 112°15′10″	Syenogranite	115 ± 2	Zircon U-Pb SHRIMP	Mao *et al.* (2010)
FN-63	Funiushan	N 33°46′25″ E 112°09′25″	Monzogranite	115 ± 1	Zircon U-Pb LA-ICPMS	Gao *et al.* (2014a)
TSM-31	Taishanmiao	N 33°51′24″ E 112°09′46″	Syenogranite	125 ± 2	Zircon U-Pb LA-ICPMS	Gao *et al.* (2014b)
Jialou area						
ZG03-1	Leshan	N 32°51′23″ E 113°53′11″	Monzogranite	130 ± 1	Zircon U-Pb LA-ICPMS	This study
ZG05-1	Zhugou	N 32°51′16″ E 113°43′12″	Monzogranite	128 ± 1	Zircon U-Pb LA-ICPMS	This study
ZG11-1	Mazhuang	N 32°52′23″ E 113°36′58″	Monzogranite	132 ± 1	Zircon U-Pb LA-ICPMS	This study
ZG13-1	Fengzhuang	N 32°53′13″ E 113°26′54″	Monzogranite	133 ± 1	Zircon U-Pb LA-ICPMS	This study

setting (Ding *et al*. 2011; Qi *et al*. 2012; Wang *et al*. 2013). The late Mesozoic granitoids are mainly exposed, from west to east, in the Xiaoqinling, Xiong'ershan, and Jialou areas (Table 1). These intrusions comprise a wide range of lithologies, including syenogranite, monzogranite, granodiorite, and quartz diorite, which occur both as small porphyritic bodies and large batholiths (Wang *et al*. 2011; 2013). Previous zircon geochronological studies for the granitoids in the Xiaoqinling and Xiong'ershan areas, adjacent to the Qinling Orogen, show that those plutons formed at 158–100 Ma (Figure 1(b); Mao *et al*. 2010; Wang *et al*. 2011). However, the ages of the granitoids in the Jialou area adjacent to the Tongbai Orogen have not been well constrained.

3. Sample descriptions

The Jialow granitoids adjacent to the Tongbai Orogen are located ~20 km northwest of the Biyang County, with an exposure outcrop of ~450 km^2. They occur as batholith intruded into the Xiong'er Group and Luanchuan Group and contain adundant xenoliths of banded and massive amphibolites. The granitoids are composed predominantly of medium- to fine-grained porphyritic biotite monzogranites. Mineral contents of the studied rocks for classification were recalculated by microscope-observation. Used it as a base, all the studied rocks have been plotted in the QAP diagram. These granitoids are composed chiefly alkali feldspar (35%–40%), plagioclase (25%–35%), quartz (15%–25%), biotite (5%–10%) and hornblende (1%–5%), with accessory mineral association of magnetite, zircon, apatite and titanite (Figure 2). Most of the alkali feldspar occurs as phenocrysts of up to 1–5 cm in size, and contain mineral inclusions of plagioclase, quartz, and biotite. Plagioclase is typically subhedral and contains polysynthetic twins; some plagioclase crystals have been subjected to sericitization and epidotization. Quartz is anhedral with a mosaic texture, and shows strong undulose extinction. Biotite is anhedral and displays a strong shape-preferred orientation; some biotite grains have been altered to chlorite. Most of the monzogranites display a weak gneissosity, defined by the alignment of alkali feldspar phenocrysts, fragmented quartz, and biotite, as a result of deformation.

To understand the nature and origin of the Jialou granitoids, nine samples were selected for detailed geochemical analyses. In addition, four representative samples were chosen for zircon U–Pb dating to constrain the age of magmatism. The sampling locations are shown in Figure 1(c), and are also detailed in Table 1 along with the mineralogy and measured age of each sample.

4. Analytical methods

Zircon crystals were extracted by conventional techniques, including crushing, sieving, heavy liquid separation, and hand picking under a binocular microscope. Representative zircon grains were mounted in epoxy discs and polished to expose two-thirds of the crystal widths. The internal morphology of the zircons was imaged using cathodoluminescence (CL). The zircon analyses were performed using laser ablation–multicollector–inductively coupled plasma–mass spectrometry (LA-MC-ICP-MS) at the Tianjin Institute of Geology and Mineral Resources, Tianjin, China. For details of the instrumental conditions and analytical procedures, see Li *et al*. (2009) and Jackson *et al*. (2004), respectively. Spot diameters were set to 35 μm, laser frequency was 8–10 Hz, and plasma density was 13–14 J/cm^2. Zircon standard CJ-1 was used as an external standard for U–Pb dating, and NIST612 was analysed twice for every six analyses when determining the concentrations of Pb, U, and Th. Off-line selection and the integration of background and sample signals, time-drift corrections, and quantitative calibrations were performed using ICPMSDataCal software (Liu *et al*. 2008, 2010b). Ages and concordia diagrams were produced using the ISOPLOT 3.23 software (Ludwig 2003). Common Pb was corrected using ^{208}Pb. Age uncertainties for individual analyses are shown as one standard deviation (1σ), and calculated weighted mean ages are quoted at the 95% confidence level.

All samples for whole-rock analyses were crushed and then pulverized in an agate mill. Whole-rock major and trace element analyses were carried out at the National Research Center for Geoanalysis at the Chinese Academy of Geological Sciences, Beijing, China. Major oxides were determined using X-ray fluorescence (XRF; Rigaku-3080) after fusion of the sample powder with lithium tetraborate. Relative standard deviations are better than 5%. Trace element abundances were measured using inductively coupled plasma–mass spectrometry (ICP–MS; TJA PQ ExCell), following the method of Wang *et al*. (2003). Sample powders were digested with a mixture of HF and HNO_3 in high-pressure Teflon bombs on a hot plate for 24 h. After complete digestion, the sample solutions were evaporated to incipient dryness, refluxed with 6N HNO_3, and heated again to incipient dryness to remove

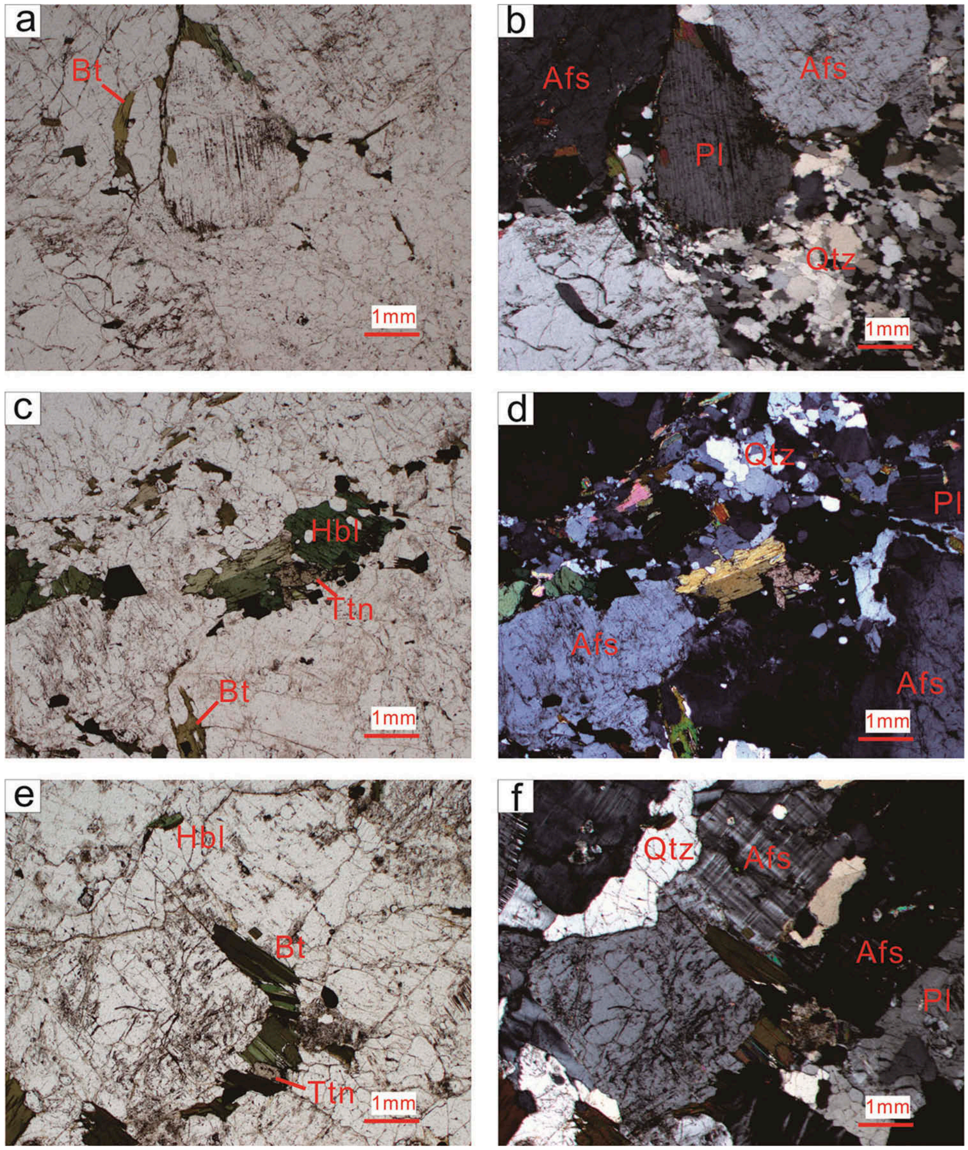

Figure 2. Photomicrographs showing the mineralogy and texyure of the Jialow granitoids. (a–b) Plagioclase with serictization forms as subhedral crystals. (c–d) Hypidiomorphic granular texture of the biotite monzogranite. (e–f) Alkali feldspar occurs as phenocryst and contains mineral inclusions of plagioclase, quartz, and biotite. Mineral abbreviations: Bt, biotite; Hbl, hornblende; Afs, alkali feldsapar; Pl, plagioclase; Qtz, quartz; Ttn, titanite.

10.1016anic matter. The samples were then dissolved in 2 ml of 3N HNO_3 and diluted with Milli-Q water (18 MX) to a final dilution factor of 2000. The detection limit for trace elements was ~0.1 ppm. Analytical uncertainties were <5% for trace elements with concentrations of ≥20 ppm, and 5%–10% for concentrations of ≤20 ppm. The chondritic values used in the normalization of rare earth element (REE) patterns and the primitive mantle (PM) values used in spider diagrams are from Sun and Mcdonough (1989).

Sr–Nd isotope analyses were conducted at the Key Laboratory of Isotopic Geology, Institute of Geology, Chinese Academy of Geological Sciences, Beijing. The Sr isotope compositions and concentrations of Rb, Sr, Sm, and Nd were measured by isotope dilution in a Finnigan MAT-262 mass spectrometer. Nd isotope compositions were acquired by a Nu Plasma HR MC-ICP-MS (Nu Instruments). The experimental procedure is described in detail by He *et al.* (2007). The Nd and Sr measurements were corrected for mass fractionation by normalization to $^{146}Nd/^{144}Nd = 0.7219$ and $^{88}Sr/^{86}Sr = 8.37521$, respectively. External precisions during this period of measurement for Sr and Nd isotopic compositions were ±0.000010 (n = 18) and ±0.000011 (n = 18), respectively. The $^{87}Sr/^{86}Sr$ ratio for the NBS987 standard is 0.710238 ± 12 (2σ) and the $^{143}Nd/^{144}Nd$ ratio for the JMC Nd standard is 0.511127 ± 10 (2σ).

5. Results

5.1. Zircon U–Pb ages

The zircon U–Pb isotopic data and representative CL images of zircons are presented in Supplementary Table 1 and Figure 3, respectively. The U–Pb concordia diagrams for the zircon analyses are shown in Figure 4. The zircons from the four samples are typically euhedral to subhedral, with short to long prismatic habits and lengths of 120–200 μm. Most of the zircons show oscillatory zoning in the CL images, as typically observed in magmatic zircons. Their Th/U ratios range from 0.04 to

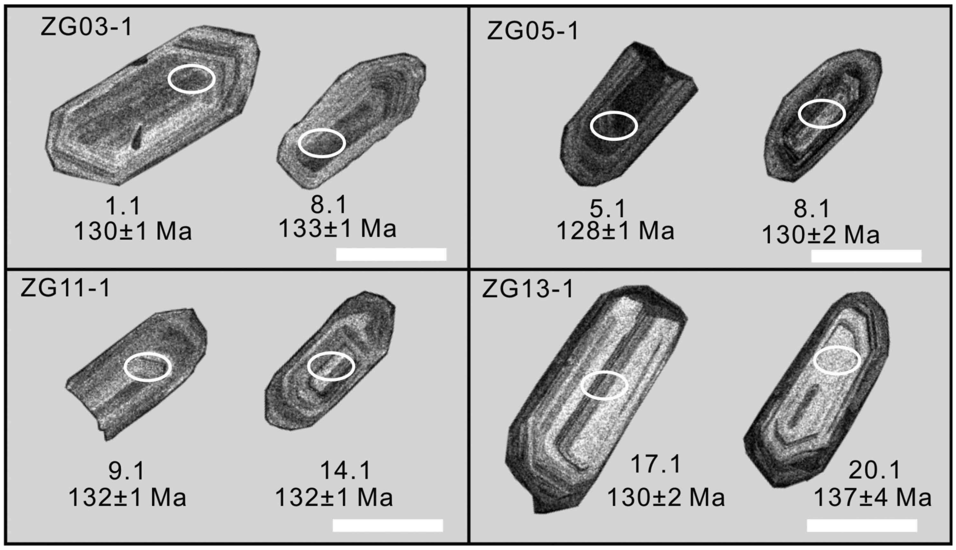

Figure 3. Representative cathodoluminescence (CL) images of zircon grains from the Jialou low-Mg adakitic rocks. The number of the sample from which the zircon was extracted is given at top left in each panel, and the analytical spots within each zircon grain are circled. Age errors are given at 1σ. Scale bars are 100 μm.

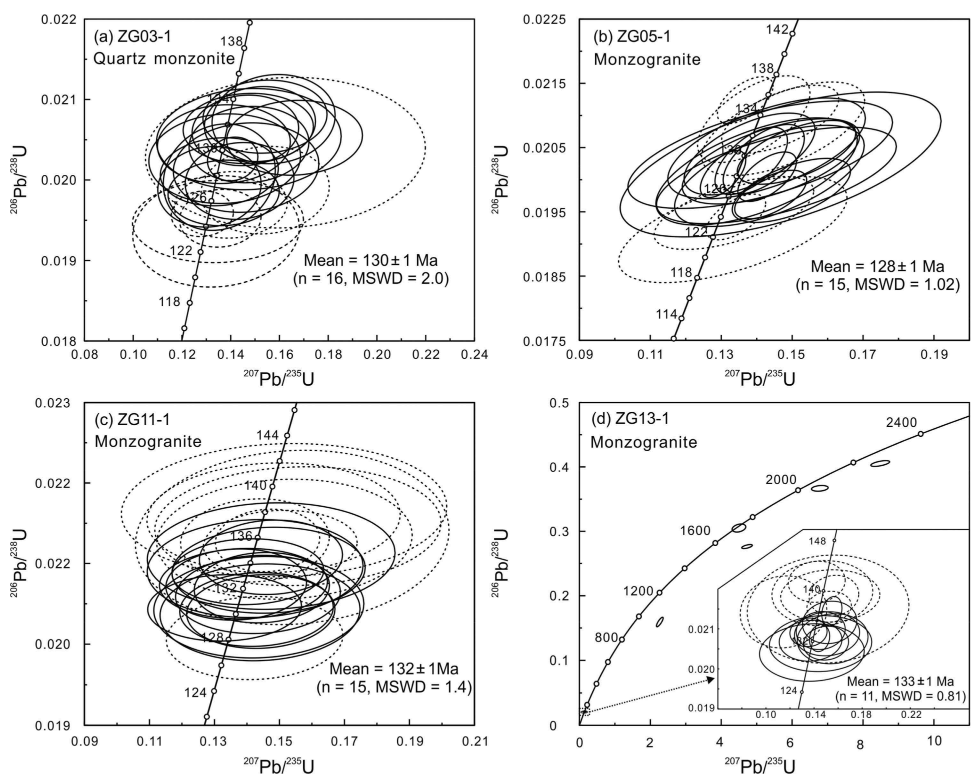

Figure 4. Zircon U–Pb concordia diagrams for selected samples of the Jialou low-Mg adakitics rocks collected along the southern margin of the NCC: (a) sample ZG03-1; (b) sample ZG05-1; (c) sample ZG11-1; (d) sample ZG13-1. See text for explanation.

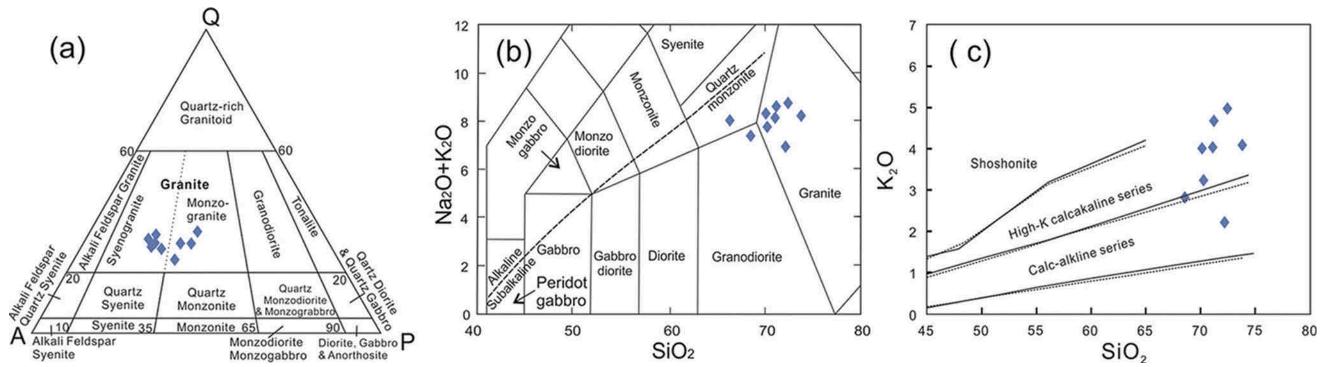

Figure 5. (a) Quartz–alkali feldspar–plagioclase (QAP) diagram of the Jialou granitoids (after Streckeisen 1976). (b) Total alkali vs. SiO_2 (TAS) diagram for classification of the Jialou granitoids (after Middlemost 1994). (c) SiO_2 vs. K_2O diagram for the Jialou granites. See text for explanation.

3.21 (mostly >0.4), also suggesting a magmatic origin (Belousova *et al*. 2002). Some captured zircons were observed in sample ZG13-3, and these have no clear oscillatory zoning.

Twenty-four analytical spots on 24 zircon grains from sample ZG03-1 yield $^{206}Pb/^{238}U$ apparent ages of between 124 ± 1 and 133 ± 1 Ma. Except for 8 outliers, the other 16 analyses yield a weighted mean age of 130 ± 1 Ma (MSWD = 2.0). Twenty-two analytical spots on 22 zircon grains from sample ZG05-1 have $^{206}Pb/^{238}U$ apparent ages ranging from 123 ± 2 to 133 ± 2 Ma. Except for 7 outliers, the other 15 analyses yield a weighted mean age of 128 ± 1 Ma (MSWD = 1.02). Twenty-three spots on 23 zircon grains from sample ZG11-1 have $^{206}Pb/^{238}U$ apparent ages ranging from 130 ± 1 to 138 ± 2 Ma. Except for 9 outliers, the other 15 analyses yield a weighted mean age of 132 ± 1 Ma (MSWD = 1.4). Twenty-four analytical spots on 23 zircon grains were analysed in sample ZG13-1. Eighteen of the analyses cluster close to the concordia curve, yielding $^{206}Pb/^{238}U$ apparent ages ranging from 130 ± 1 to 138 ± 2 Ma. Except for 7 outliers, the other 11 analyses yield a weighted mean age of 133 ± 1 Ma (MSWD = 0.81). The remaining five analyses yield concordant $^{207}Pb/^{206}Pb$ ages of 1751 ± 32 Ma, 2017 ± 22 Ma, 2368 ± 21 Ma, 2153 ± 24 Ma, and 1683 ± 24 Ma, representing the ages of captured zircons. Thus, our above zircon U–Pb isotopic dating results reveal that the Jialou granitoids were emplaced at ~130 Ma.

5.2. Major and trace elements

The major and trace element data for the Jialou granitoids are listed in Supplementary Table 2. In the quartz–alkali feldspar–plagioclase (QAP) diagram, all the samples are plotted in the field of granite (Figure 5(a)). All the samples have similar geochemical compositions to each other. They have high contents of SiO_2 (66.39–73.83 wt.%), K_2O (2.21–4.97 wt.%), Al_2O_3 (13.91–15.50 wt.%), Sr (452–688 ppm), and Ba (918–2168 ppm), high ratios of Sr/Y (34–78) and $(La/Yb)_N$ (21–43, except for sample ZG03-1), and low concentrations of MgO (0.26–1.5 wt.%) and low $Mg^{\#}$ (<45, with three exceptions). They are all subalkaline according to the total alkaline vs. silica (TAS) classification of Middlemost (1994) (Figure 5(b)). In the K_2O vs. Si_2O classification diagram the samples plot in the high-K calc-alkaline field (Figure 5(c)). The Jialou monzogranites are metaluminous to weakly peraluminous with A/NCK ratios [molar $Al_2O_3/(CaO+Na_2O+K_2O)$] of 0.93–1.04. In the chondrite–normalized REE patterns, these samples have been found to be significantly enriched in light rare earth elements (LREE) and strongly depleted in heavy rare earth elements (HREE), with $(La/Yb)_N$ = 13–43 (Figure 6(a)). They have a total REE contents of 95–292 ppm and minor or no negative Eu anomalies (Eu/Eu* = 0.72–0.99). In N-MORB-normalized spider diagrams (Figure 6(b)), they are characterized by enrichment of large ion lithophile elements (LILE; e.g. Rb, Sr, Ba, Th, and U) and depletion of high field strength elements (HFSE; e.g. Nb, Ta, and Ti) and P.

5.3. Whole-rock Sr–Nd isotopes

Whole-rock Rb–Sr and Sm–Nd isotope data for rocks from the Jialou granitoids are presented in Supplementary Table 3 and plotted in Figure 7. The initial $^{87}Sr/^{88}Sr$ and $^{144}Nd/^{143}Nd$ ratios were calculated at 130 Ma on the basis of zircon U–Pb dating of the monzogranites. Four monzogranite samples display similar isotopic compositions with initial $^{87}Sr/^{86}Sr$ (I_{Sr}) ratios of 0.707464–0.70819 and $\varepsilon_{Nd}(t)$ values of −11.8 to −15.2. These samples have Nd two-stage model ages (T_{DM2}) of 1.9–2.2 Ga.

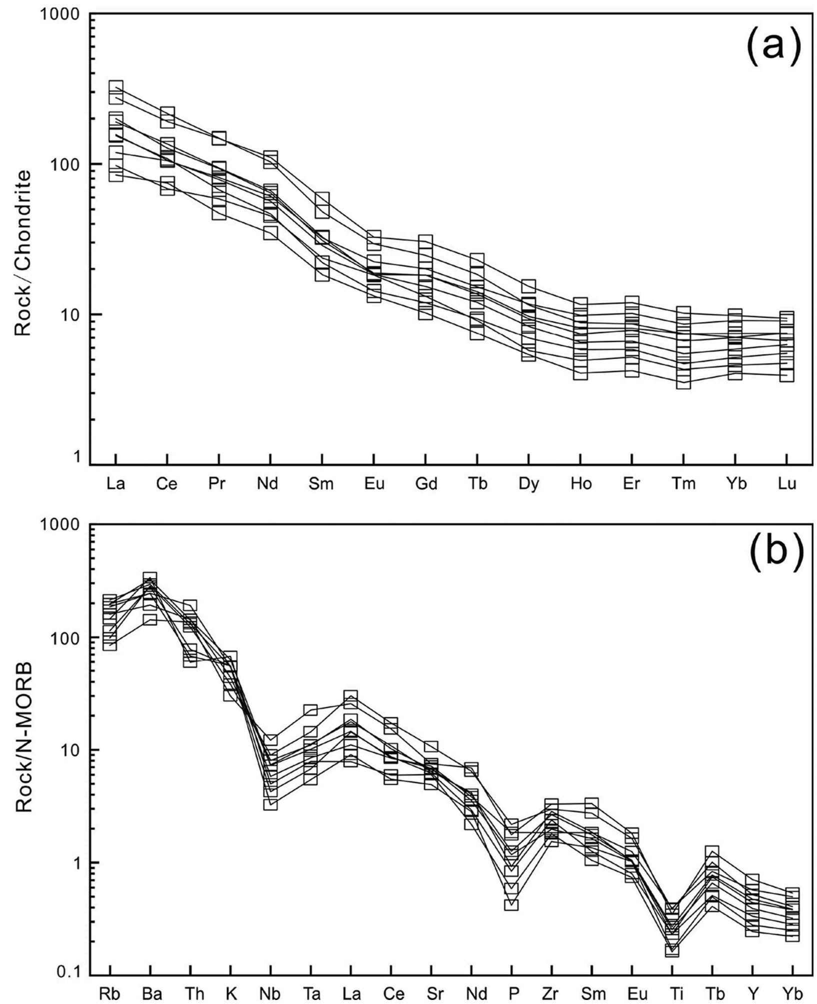

Figure 6. (a) Chondrite–normalized REE pattern and (b) N-MORB–normalized trace element spider diagrams for the Jialou granitoids. Chondrite and N-MORB values used for normalization are from Sun and Mcdonough (1989).

6. Discussion

6.1. Petrogenesis of the adakitic granites

The Jialou granitoids have high SiO_2, Al_2O_3, K_2O, and Sr contents (>400 ppm), and high ratios of Sr/Y (34–78) and $(La/Yb)_N$ (21–30, except for sample ZG03-1), as well as low Y (7.99–20.2 ppm) and Yb (0.78–1.67 ppm) contents (Supplementary Table 2). Most samples fall within the adakite field in the Sr/Y vs. Y diagram (Figure 8). Moreover, their REE patterns show strong LREE enrichment and negligible Eu anomalies (Figure 6(a)). All these geochemical characteristics indicate that the granitoids are most likely low-Mg adakitic rocks, similar to the late Mesozoic low-Mg adakitic rocks in the Dabie Orogen (Wang *et al*. 2007a; H.J. Xu *et al*. 2007; 2012; He *et al*. 2011). Several mechanisms have been proposed for the origin of adakites and adakitic rocks: (1) partial melting of subducted basaltic oceanic crust (Drummond and Defant 1990; Martin 1999; Yogodzinski *et al*. 2001); (2) partial melting of thickened lower continental crust (Atherton and Petford 1993; Petford and Atherton 1996; Smithies and Champion 2000; Wang *et al*. 2006); (3) partial melting of delaminated lower continental crust (Xu *et al*. 2002; Gao *et al*. 2004; Wang *et al*. 2006; W.L. Xu *et al*. 2006; Hou *et al*. 2007); and (4) assimilation and fractional crystallization (AFC) processes from parental basaltic magmas (Feeley and Hacker 1995; Wareham *et al*. 1997; Castillo *et al*. 1999; Macpherson *et al*. 2006).

The final collision of the NCC and the Yangtze Craton (YC) occurred in the late Permian–Triassic, followed by crustal extension and lithospheric thinning in the Early Cretaceous (Ames *et al*. 1993, 1996; Li *et al*. 1993; Liu *et al*. 2011, 2013; Wu and Zheng 2013). The Jialou adakitic rocks along the southern margin of the NCC were formed in an interior continental setting during the Cretaceous. Compared with typical adakites formed by partial melting of subducted oceanic crust, they have

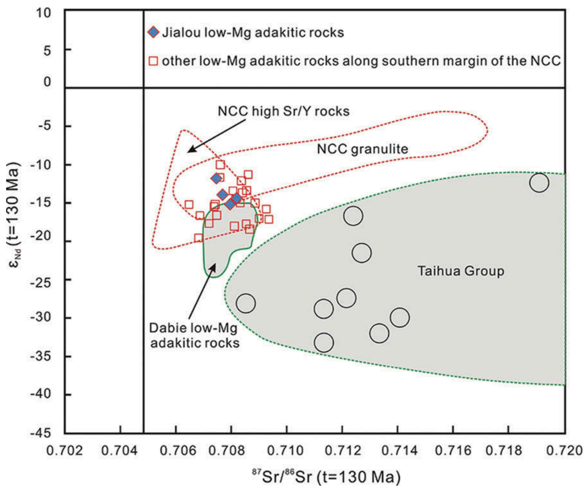

Figure 7. Nd–Sr isotopic compositions of the Jialou adakitic rocks. Other low-Mg adakitic rocks along the southern margin of the NCC are from Guo *et al.* (2009), Zhao *et al.* (2012a), Hu *et al.* (2012), and Li *et al.* (2013). The data for NCC high-Sr/Y rocks (which are Early Cretaceous in age) are from W.L. Xu *et al.* (2006, 2008); Hou *et al.* (2007); Wu *et al.* (2005); and Jiang *et al.* (2007), representing the lower crust of the NCC. The data for NCC granulites are from Zhou *et al.* (2002) and Liu *et al.* (2004). The data for Dabie low-Mg adakitic rocks (which are Early Cretaceous in age) are from Chen *et al.* (2002), Zhang *et al.* (2002), Wang *et al.* (2007a), H.J. Xu *et al.* (2012), and He *et al.* (2013). The data for the Taihua Group are from Huang and Wu (1990), Ni *et al.* (2009), and X.S. Xu *et al.* (2009).

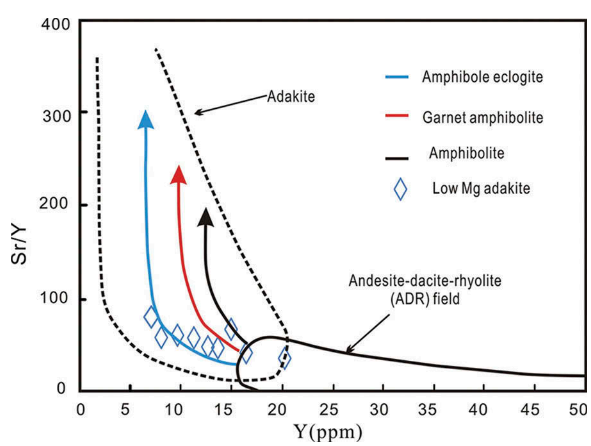

Figure 8. Sr/Y vs. Y diagram for the Jialou adakitic rocks. Fields of adakite and arc magmatic rocks are from Drummond and Defant (1990).

higher K_2O contents (2.21–4.97 wt.%) and initial $^{87}Sr/^{86}Sr$ ratios, lower $Mg^{\#}$ (<45), and lower $^{143}Nd/^{144}Nd$ ratios. These properties preclude the possibility of derivation from partial melting of subducted oceanic slab.

Castillo *et al.* (1999) proposed that adakitic rocks can be produced by low-pressure fractionation of amphibole from basaltic magma. Variable fractionation of amphibole could theoretically cause an increase in the Sr/Y and La/Yb ratios (Zhao and Zhou 2007). Therefore, one could infer that the high Sr/Y ratios are the result of such a process. However, the adakitic rocks produced by fractionation of amphibole should have U-shaped chondrite-normalized REE patterns and variable Dy/Yb ratios (Macpherson *et al.* 2006). The right-inclined REE pattern and constant Dy/Yb ratios of the adakitic rocks studied here are therefore inconsistent with an origin by fractional crystallization of amphibole (Figure 6(a)). Their Sr/Y and La/Yb ratios have no obvious correlations with SiO_2, also suggesting that high Sr/Y and La/Yb ratios were inherited from the source region, rather than produced by magma differentiation. In addition, co-existing Cretaceous basalt or gabbro has not been found in the Jialou area, further excluding the possibility that the adakitic rocks in the region are a product of fractional crystallization.

In general, magmas that form by partial melting of delaminated lower continental crust subsequently interact with mantle peridotite during ascent (Gao *et al.* 2004). Therefore, adakitic rocks derived from delaminated lower continental crust typically have higher MgO, Cr, and Ni contents, and $Mg^{\#}$ values than those formed directly from thickened lower continental crust (e.g. W.L. Xu *et al.* 2006, 2008; Huang *et al.* 2008; Zhang *et al.* 2010; Yu *et al.* 2015). However, the Jialou adakitic rocks show low MgO, Cr, and Ni contents and $Mg^{\#}$ values. In the SiO_2 vs. MgO diagram (Figure 9), all samples plot in the field of adakitic rocks derived from partial melting of mafic lower crust and experimental melts of metabasalts and eclogites at 1–4.0 GPa. The geochemical characteristics above are similar to those of the Early Cretaceous low-Mg adakitic rocks in the Dabie Orogen and along the southern margin of the NCC, both of which are thought to be derived from melting of the thickened lower crust (Chen *et al.* 2002; Wang *et al.* 2007a; H.J. Xu *et al.* 2007; 2012; He *et al.* 2011; 2013; Hu *et al.* 2012; Li *et al.* 2012, 2013; Zhao *et al.* 2012a; Yang *et al.* 2010; 2016). Hence, the partial melting of thickened lower crust is a plausible explanation for the generation of the low-Mg adakitic rocks in the Jialou area adjacent to the Tongbai Orogen.

6.2. Nature of the magmatic source

The low-Mg adakitic rocks in the Jialou area have relatively high initial $^{87}Sr/^{86}Sr$ ratios (0.7075–0.7082) and negative $\varepsilon_{Nd}(t)$ values (−11.8 to −15.2), similar to other Early Cretaceous low-Mg adakitic rocks in the southern margin of the NCC ($(^{87}Sr/^{86}Sr)_i$ = 0.7074–0.7089, $\varepsilon_{Nd}(t)$ = −10.1 to −18.5; Hu *et al.* 2012; Zhao *et al.* 2012a; Li *et al.* 2013) (Figure 7). This similarity suggests that all Early

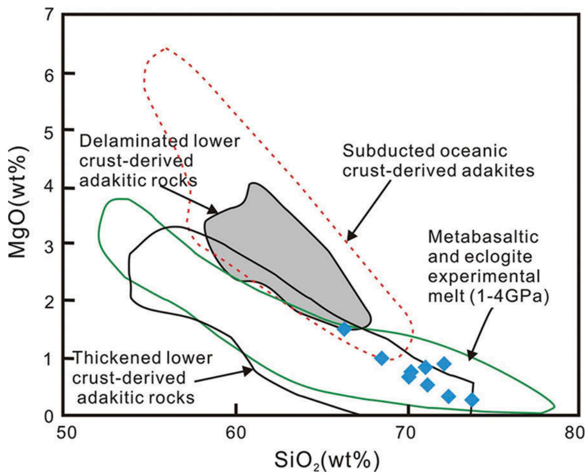

Figure 9. MgO vs. SiO_2 diagram (after Wang *et al.* 2006) for the Jialou adakitic rocks. Field of thickened lower crust–derived adakitic rocks are from Atherton and Petford (1993), Petford and Atherton (1996), and Smithies and Champion (2000) Wang *et al.* (2006). Field of experimental melts of metabasalt and eclogite obtained at pressures of 1.0–4.0 GPa are from Rapp *et al.* (1991), Sen and Dunn (1994), Rapp and Watson (1995), and Springer and Seck (1997). Field of the subducted oceanic crust–derived adakities are from Drummond and Defant (1990) Martin (1999) and Yogodzinski *et al.* (2001). Field of delaminated lower crust–derived adakitic rocks are from J.F. Xu *et al.* (2002), Gao *et al.* (2004), and Wang *et al.* (2006).

Cretaceous low-Mg adakitic rocks along the southern margin of the NCC were derived from the same source. Their whole-rock two-stage Nd model ages range from 1.9 to 2.2 Ga, suggesting that a Palaeoproterozoic lower crust was the major source of the adakitic rocks. However, it is still unclear whether the lower crust was derived from the NCC or the subducted YC, because the YC was subducted beneath the southern margin of the NCC during or before the Late Jurassic (Ames *et al.* 1993, 1996; Li *et al.* 1993; Liu *et al.* 2011, 2013; Wu and Zheng 2013; Yang *et al.* 2016). Zircon U–Pb dating results of the Jialou adakitic rocks do not show any Neoproterozoic and Triassic ages. This feature had been proved by zircon U–Pb dating results of the other Early Cretaceous adakitic rocks in the southern margin of the NCC (Zhao *et al.* 2012a; Hu *et al.* 2012., Li *et al.* 2012, 2013). Instead, the predominately late Archean to Palaeoproterozoic inherited zircons suggest that the adakitic magmas that produced these rocks were derived from partial melting of ancient NCC basement material. Additionally, the Sr–Nd isotopic compositions of the Jialou adakitic rocks are similar to those of the adakitic rocks along the eastern margin of the NCC, which were derived from partial melting of the mafic lower crust of the NCC (W.L. Xu *et al.* 2006, 2008, Hou *et al.* 2007; Jiang *et al.* 2007; Yang *et al.* 2010, 2016), but are distinct from low-Mg adakitic rocks in the Dabie Orogen, which were derived from partial melting of the lower crust of the YC (Chen *et al.* 2002; Zhao *et al.* 2005b; 2007; Wang *et al.* 2007a; H.J. Xu *et al.* 2007; 2012; He *et al.* 2011; 2013) (Figure 7). Thus, it can be concluded that the Early Cretaceous adakitic rocks in the Jialou area were most likely directly derived from partial melting of the ancient lower crust of the NCC.

The widespread Taihua Group basement rocks are the oldest rocks along the southern margin of the NCC. They have been metamorphosed to the amphibolite facies, and locally to the granulite facies, consistent with middle- to lower-crustal levels (Rudnick and Fountain 1995, Rudnick and Gao 2003). Available geochronological data show that the Taihua Group was formed mostly during the Neoarchean and Palaeoproterozoic (2.84–2.26 Ga), and was strongly deformed and metamorphosed between 2.1 and 1.8 Ga (Kröner *et al.* 1988; Xue *et al.* 1995; Wan *et al.* 2006; Xu *et al.* 2009). However, the initial $^{87}Sr/^{86}Sr$ and $\varepsilon_{Nd}(t)$ values of the Neoarchean and Palaeoproterozoic Taihua Group metamorphic basement rocks at the age of intrusion (~130 Ma) are distinct from those of the adakitic rocks in the Jialou area (Figure 7). Furthermore, the whole-rock two-stage Nd model ages (1.9–2.2 Ga) of adakitic rocks are much younger than the ages of the Taihua Group. Hence, the Taihua Group may not be the magma source of the Jialou adakitic rocks. Granulite xenoliths brought to the surface by basaltic volcanics and kimberlites provide an ideal opportunity to study samples of the lower continental crust (Rudnick and Fountain 1995; Rudnick and Gao 2003). Granulite xenoliths entrained within the Mesozoic Xinyang volcaniclastic diatremes in the southern NCC reveal that the lower crust there was strongly influenced by a tectono-thermal event during the Palaeoproterozoic (1.8–2.2 Ga) (Zheng *et al.* 2003, 2004a, 2006, 2008; Ping *et al.* 2015), corresponding to the timing of the collision between the eastern and western blocks of the NCC (Zhao *et al.* 2000, 2005a, 2012b; Santosh *et al.* 2007; Santosh 2010). The geochemical characteristics and Hf isotope compositions of zircons from 1.8–2.1 Ga intermediate and mafic granulites from the lowermost part of the lower crust suggest that they were the products of mantle-derived magma that was underplated and contaminated by older crustal components (Zheng *et al.* 2003, 2008). The Palaeoproterozoic (1.8–2.2 Ga) tectono-thermal event is also recorded in granulite xenoliths from the Hannuoba basalts at the northern edge of the Trans-North China Orogen and the Fuxian kimberlites in the eastern part of the Eastern Block (Zheng *et al.* 2004a, 2004b; Zhang *et al.* 2012; Tang *et al.* 2014). The widespread evidence for a magmatic/thermal event at this time demonstrates the presence of a 1.8–2.2 Ga lower crust, which may be the most likely source of the Jialou adakitic rocks. Moreover, the 1.8–2.2 Ga intermediate and mafic granulites have Sr–Nd isotopic compositions that are indistinguishable from those of the Jialou adakitic rocks (Figure 7), indicating that the adakitic rocks in the Jialou area were derived from partial melting of the 1.8–2.2 Ga lower crust of the NCC.

The geochemical compositions of melts are thought to be buffered by equilibrated residues (Rapp *et al*. 1991; Sen and Dunn 1994; Springer and Seck 1997; Litvinovsky *et al*. 2000). Garnet is strongly compatible for HREEs (e.g. Yb and Lu) (Nash and Crecraft 1985; Otamendi *et al*. 2002), and amphibole is compatible for MREEs and HREEs (e.g. Dy and Ho) and Y. When garnet is the main residual mineral, HREE plots will show steep patterns with Y/Yb > 10 and $(Ho/Yb)_N > 1.2$ (Ge *et al*. 2002; Hu *et al*. 2012). In contrast, when amphibole is the main residual mineral phases, HREE plots will show flat patterns with Y/Yb ≈ 10 and $(Ho/Yb)_N \approx 1$ (Ge *et al*. 2002; Hu *et al*. 2012). Ca-rich plagioclase has a high partition coefficient for Sr and Eu (Nash and Crecraft 1985), and thus crystallization of Ca-rich plagioclase in melt residues can result in depletions of Sr and Eu in the equilibrium melt. The Jialou low-Mg adakitic rocks have much high Sr, Sr/Y, and $(La/Yb)_N$ ratios, and lower Y (Supplementary Table 2), and they show flat HREE patterns with Y/Yb and $(Ho/Yb)_N$, and negligible negative Eu anomalies (Figure 6, Supplementary Table 3). This indicates that garnet and amphibole, but little or no plagioclase, were residual phases in the source of the Jialou adakitic rocks. In addition, geochemical modelling of Sr/Y vs. Y (Figure 8) shows that the Jialou adakitic rocks could have been derived by partial melting of a basaltic source, resulting in an eclogite to garnet amphibolite residual phase (Drummond and Defant 1990).

6.3. Implications for crustal evolution

As already discussed above, the Early Cretaceous Jialou adakitic rocks were most likely derived from partial melting of a thickened mafic lower crust containing the residual phases of eclogites and amphibolites. Partial melting experiments on mafic rocks indicate that garnet becomes stable at depths of at least 40 km (12 kbar), and more typically, greater than 50 km (15 kbar), while plagioclase becomes unstable at depths greater than ~50 km (15 kbar) (Sen and Dunn 1994; Rapp 1995; Rapp and Watson 1995; Litvinovsky *et al*. 2000; Patiño Douce 2005). Therefore, the Early Cretaceous Jialou adakitic rocks with pronounced garnet and amphibole signatures, but without plagioclase fingerprints in their sources, were formed by partial melting of mafic lower crust at pressures greater than 15 kbar, suggesting that a thick (>50 km) crustal root was present under the southern margin of the NCC during the Early Cretaceous. The widespread Late Jurassic to Early Cretaceous adakitic granites (160–135 Ma) along the southern margin of the NCC, adjacent to the Qinling Orogen, also imply a crustal thickness of ~50 km during the Late Jurassic to Early Cretaceous (Guo *et al*. 2009; Hu *et al*. 2012; Li *et al*. 2012; Zhao *et al*. 2012a; Li *et al*. 2013). The lower-crustal mafic xenoliths from the Mesozoic (~160 Ma) volcaniclastic diatreme in Xinyang, along the southern margin of the NCC and adjacent to the Tongbai Orogen, indicate that the Late Jurassic lower crust extended to at least 41–56 km depth (Zheng *et al*. 2003). However, the Late Triassic (228–215 Ma) shoshonitic granitoids along the southern margin of the NCC (Ding *et al*. 2011; Qi *et al*. 2012) have much higher HREE contents and lower La/Yb ratios than the Early Cretaceous adakitic rocks, suggesting that crustal thickness was less than 40 km in the Late Triassic. Thus, the crust was considerably thickened during the Late Triassic to Late Jurassic. Previous studies have suggested that the crustal thickening was related to the Triassic collision between the North China and Yangtze cratons (W.L. Xu *et al*. 2006; 2008; H.J. Xu *et al*. 2007; Wang *et al*. 2007a; Guo *et al*. 2009; Li *et al*. 2013b; Liu *et al*. 2012; Yang *et al*. 2016). However, the geochronological and geochemical characteristics of the Triassic (228–200 Ma) granitoids in the Qinling Orogen suggest a setting of post-collisional extension during the Late Triassic (Wang *et al*. 2005, 2007b, 2011, 2013; Zhang *et al*. 2005; Qin *et al*. 2009; Ding *et al*. 2011). Meanwhile, the geochronology data and P–T paths of the HP–UHP metamorphic rocks in the Qinling–Tongbai–Dabie Orogen suggest that the continental deep subduction slabs were exhumed to mid-crustal levels in the Late Triassic (Hacker *et al*. 1998; Zheng *et al*. 2002; Liu *et al*. 2010a, 2011). Therefore, the crustal thickening and magmatism after the Late Triassic was not connected with the NCC–YC collisional events. Given the lack of Jurassic (200–160 Ma) magmatism along the southern margin of the NCC and the Qinling–Tongbai–Dabie Orogen, crustal thickening is unlikely to have been caused by the underplating of mantle-derived magma. This consideration is also supported by the εNd(t) values (−11.8 to −15.2) of the Jialou granitoids. Studies of late Mesozoic deformation and magmatism in the east continent indicate that strong intra-continental orogenesis and crustal thickening occurred during the late Middle Jurassic to Early Cretaceous, which resulted from multi-directional contraction due to the far-field effects of multiple plate convergence and related orogenic activities (the collisional north Mongol–Okhotsk Orogen, the accretionary coastal Orogen along the eastern margin of the east Asian continent, the Bangong–Nujiang Orogen in the southwest) around the east Asian continent (Davis *et al*. 2001; Dong *et al*. 2007, 2008, 2015; Zhang *et al*. 2007; Li *et al*. 2013a; W.L. Xu *et al*. 2013). The lithosphere of the east Asian continent was thickened, reaching a maximum during the Late Jurassic or the Early Cretaceous. Based on the above considerations, we consider that crustal thickening along the southern margin of the NCC was caused by a Middle Jurassic to Early Cretaceous intra-continental orogeny.

The Jialou adakitic rocks suggest that the thickened crust (>50 km) beneath the southern margin of the NCC still existed at 130 Ma or younger. In Cenozoic basalts from the NCC, eclogite xenoliths are absent and high-pressure granulite xenoliths do not contain garnet, indicating that the Cenozoic crust was significantly thinner than the Mesozoic crust (Zheng *et al*. 2003). The late-stage Early Cretaceous (<130 Ma) granites have low $(La/Yb)_N$ and Sr/Y ratios, and significantly negative Eu anomalies, suggesting that their parental magmas were in equilibrium with residues containing plagioclase, hornblende, and no garnet (Gao *et al*. 2014a, 2014b). These late-stage granites were formed by partial melting of the crustal root at depths of less than 40 km, implying that the high-density granulitic and eclogitic lower crust during the early stage of the Early Cretaceous was delaminated prior to emplacement of the late-stage granites. Therefore, the thickened crust must have been rapidly thinned after the formation of the adakitic rocks (~130 Ma). A similar magmatic evolution and thinning of thickened crust have been found in the Dabie–Sulu Orogen, the Xuhuai area, the Jiaodong peninsula, the Liaodong area, and the interior of the NCC (Yang *et al*. 2005; W.L. Xu *et al*. 2006; Hou *et al*. 2007; He *et al*. 2011; 2013; Guo *et al*. 2013; Li *et al*., 2013; Zhang *et al*. 2013; Yang *et al*. 2016). We therefore suggest that the late Mesozoic adakitic magmas in the NCC were controlled by a uniform tectonic regime. Recently, an increasing number of studies have suggested that the westward subduction of the Palaeo-Pacific plate beneath the east Asian continental margin played an important role in the Early Cretaceous magmatism and lithospheric thinning of the NCC (Guo *et al*. 2013; Tang *et al*. 2013; Goldfarb and Santosh 2014; Gao *et al*. 2014a, 2014b). Consequently, the crustal thinning corresponding to the lithospheric thinning of the NCC in the Early Cretaceous may have been related to subduction of the Palaeo-Pacific plate.

Based on the discussions above, we propose the following scenario to explain the late Mesozoic crustal evolution and magmatic activities of the southern margin of the NCC (Figure 10). In the Early to Middle Triassic, the NCC collided with the YC along the Qinling–Tongbai–Dabie Orogen, following the subduction of Palaeo-Tethyan oceanic crust. Until the Late Triassic, the subducted slab break-off might cause upwelling of the asthenospheric mantle. The asthenospheric upwelling induced partial melting of the enriched lithospheric mantle and lower crust, and led to the formation of post-collision granitoids. The tectonic setting gradually changed from collision compression to post-collision relaxation. Following a quiet period of magmatism (200–160 Ma), the late Middle Jurassic to Early Cretaceous intra-continental orogenesis thickened the lithosphere of the southern margin of the NCC. The thickened lithospheric keel dipped into the hot asthenosphere. The convection of deep (hot) asthenosphere might have reactivated the lithospheric keel, elevating the geothermal gradient of lithosphere and reducing partial melting of the pre-existing thickened lower crust to generate large amounts of adakitic granitoids in the 160–130 Ma. Partial melting of the thickened lower crust would increase the density of the lower crust and trigger the delamination and foundering of the residues of lower crust and underlying lithospheric mantle after 130 Ma. Meanwhile, the input of heat sources from the upwelling asthenosphere induced widespread partial melting of the thinned crust, generating normal granitoid rocks. The continental crust of the southern margin of the NCC must have been thinned after the extraction of the adakitic magmas and the delamination of the lower crust and lithospheric mantle.

7. Conclusions

(1) The Jialou granitoids along the southern margin of the NCC, adjacent to the Tongbai Orogen, were emplaced at ~130 Ma and have high Sr and Ba contents, high Sr/Y and $(La/Yb)_N$ ratios, and low MgO and Y concentrations, indicating a low-Mg adakitic affinity.

(2) The Jialou low-Mg adakitic rocks were derived from partial melting of mafic Palaeoproterozoic (1.8–2.2 Ga) lower crust of the NCC at depths of >50 km, leaving the residual phases of garnet and amphibolite.

(3) The crustal thickening during the late Middle Jurassic to Early Cretaceous and crustal thinning after 130 Ma along the southern margin of the NCC were not directly related to the collision between the North China and Yangtze cratons.

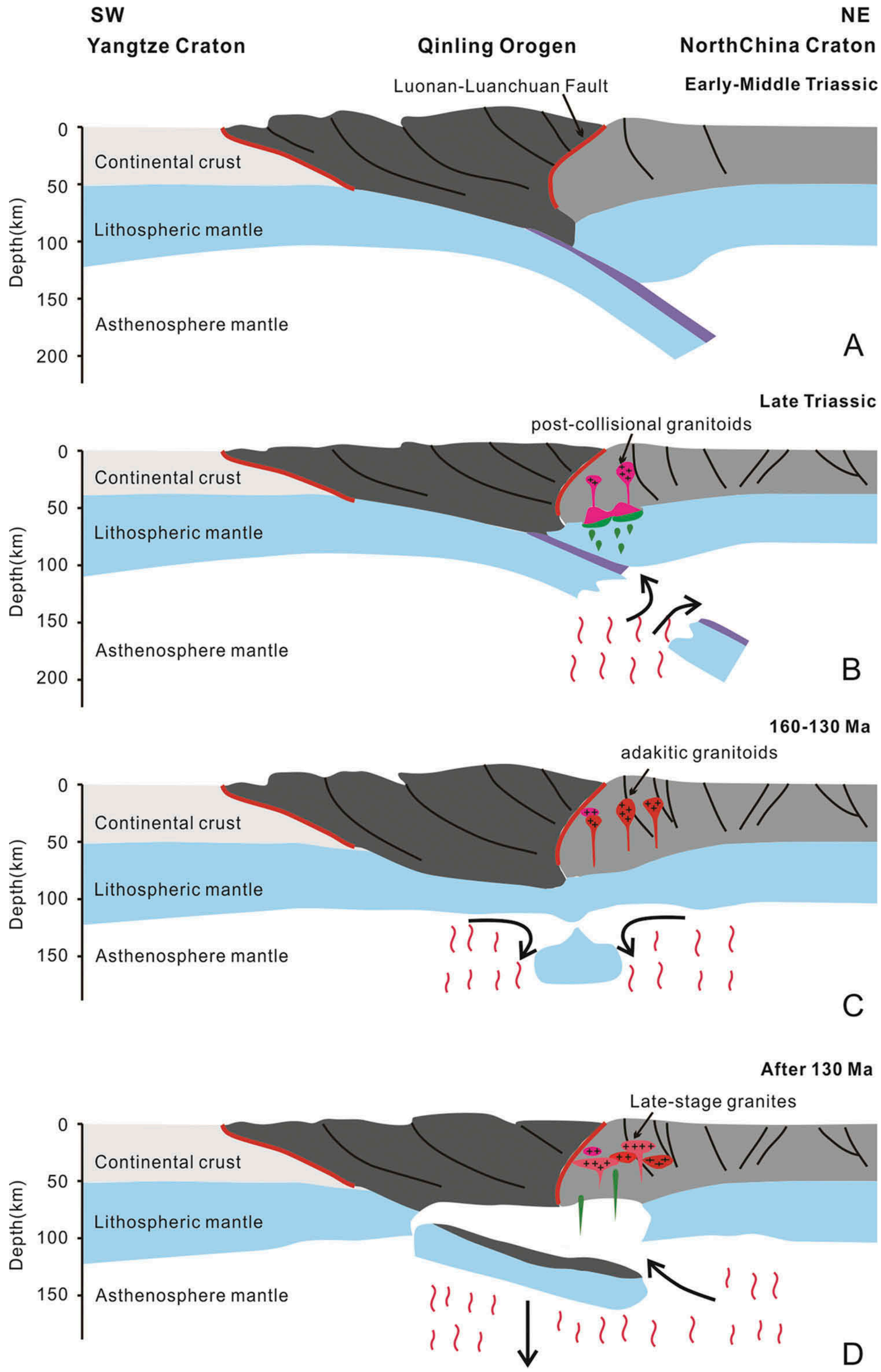

Figure 10. Cartoons showing the Mesozoic crustal evolution and magmatic activities of the southern margin of the North China Craton. (a) Early–Middle Triassic: Continental collision between the Yangtze and North China Cratons during the Early to Middle Triassic. (b) Late Triassic: Slab break-off caused upwelling of the asthenosphere in the Late Triassic and partial melting of enriched lithospheric mantle and lower crust, forming the post-collision granitoids (modified from Ding *et al*. 2011). (c) 160–130 Ma: Convection of hot asthenosphere might have reactivated the lithospheric keel, elevating the geothermal gradient of lithosphere and reducing partial melting of the thickened lower crust to generate large amounts of adakitic granitoids. (d) After 130 Ma: Foundering of the residues of lower crust and underlying lithospheric mantle resulted in asthenospheric upwelling leading to partial melting of the thinned crust, producing massive normal granitoids.

Acknowledgments

We sincerely acknowledge Huaikun Li and Jianzhen Geng for assistance in the LA-MC-ICP-MS U–Pb zircon analyses. Critical reviews by two anonymous reviewer and Editor-in-Chief's comments by Dr Robert J. Stern substantially improved the manuscript. This research was supported by the National Key Basic Science Research Project of China [grant number 2015CB856104] and the National Natural Science Foundation of China [grant number 41472064].

Disclosure statement

No potential conflict of interest was reported by the authors.

Funding

This work was supported by the National Key Basic Science Research Project of China [grant number 2015CB856104], National Natural Science Foundation of China [grant number 41472064].

References

Ames, L., Tilton, G.R., and Zhou, G.Z., 1993, Timing of collision of the Sino-Korean and Yangtse cratons: U-Pb zircon dating of coesite-bearing eclogites: Geology, v. 21, p. 339–342. doi:10.1130/0091-7613(1993)021<0339:TOCOTS>2.3.CO;2

Ames, L., Zhou, G., and Xiong, B., 1996, Geochronology and isotopic character of ultrahigh–pressure metamorphism with implications for collision of the Sino-Korean and Yangtze Cratons, central China: Tectonics, v. 15, p. 472–489. doi:10.1029/95TC02552

Atherton, M.P., and Petford, N., 1993, Generation of sodium-rich magmas from newly underplated basaltic crust: Nature, v. 362, p. 144–146. doi:10.1038/362144a0

Belousova, E.A., Griffin, W.L., Reilly, S.Y.O., and Fisher, N.I., 2002, Igneous zircon: Trace element composition as an indicator of source rock type: Contributions to Mineralogy and Petrology, v. 143, p. 602–622. doi:10.1007/s00410-002-0364-7

Castillo, P.R., Janney, P.E., and Solidum, R.U., 1999, Petrology and geochemistry of Camiguin Island, southern Philippines: Insights to the source of adakites and other lavas in a complex arc setting: Contributions to Mineralogy and Petrology, v. 134, p. 33–51. doi:10.1007/s004100050467

Chen, B., Jahn, B.M., and Wei, C.J., 2002, Petrogenesis of Mesozoic granitoids in the Dabie UHP complex, Central China: Trace element and Nd–Sr isotope evidence: Lithos, v. 60, p. 67–88. doi:10.1016/S0024-4937(01)00077-9

Chen, Y.J., 2006, Orogenic-type deposits and their metallogenic model and exploration potential: Geology In China, v. 33, p. 1181–1196. (in Chinese with English abstract).

Chen, Y.J., Chen, H.Y., Zaw, K., Pirajno, F., and Zhang, Z.J., 2007, Geodynamic settings and tectonic model of skarn gold deposits in China: An overview: Ore Geology Reviews, v. 31, p. 139–169. doi:10.1016/j.oregeorev.2005.01.001

Chen, Y.J., Guo, G.J., and Li, X., 1998, Metallogenic geodynamic background of Mesozoic gold deposits in granite–greenstone terrains of North China Craton: Science in China Series D: Earth Sciences, v. 41, p. 113–120. doi:10.1007/BF02932429

Davis, G.A., Zheng, Y.D., Wang, C., Darby, B.J., Zhang, C.H., and Gehrels, G., 2001, Mesozoic tectonic evolution of the Yanshan fold and thrust belt, with emphasis on Hebei and Liaoning Provinces, northern China: Geological Society of America Memoir, v. 194, p. 171–197.

Deng, Z.B., Liu, S.W., Zhang, W.Y., Hu, F.Y., and Li, Q.G., 2016, Petrogenesis of the Guangtoushan granitoid suite, central China: Implications for Early Mesozoic geodynamic evolution of the Qinling Orogenic Belt: Gondwana Research, v. 30, p. 112–131. doi:10.1016/j.gr.2015.07.012

Ding, L.X., Ma, C.Q., Li, J.W., Robinson, P.T., Deng, X.D., Zhang, C., and Xu, W.C., 2011, Timing and genesis of the adakitic and shoshonitic intrusions in the laoniushan complex, southern margin of the North China Craton: Implications for postcollisional magmatism associated with the Qinling Orogen: Lithos, v. 126, p. 212–232. doi:10.1016/j.lithos.2011.07.008

Dong, S.W., Zhang, Y.Q., Chen, X.H., Long, C.X., Wang, T., Yang, Z.Y., and Hu, J.M., 2008, The formation and deformational characteristics of East Asia multi-direction convergent tectonic system in Late Jurassic: Acta Geoscientica Sinica, v. 29, no. 3, p. 306–317. (in Chinese with English abstract).

Dong, S.W., Zhang, Y.Q., Long, C.X., Yang, Z.Y., Ji, Q., Wang, T., Hu, J.M., and Chen, X.H., 2007, Jurassic tectonic revolution in china and new interpretation of the Yanshan movement: Acta Geologica Sinica, v. 81, no. 11, p. 1449–1461. (in Chinese with English abstract)

Dong, S.W., Zhang, Y.Q., Zhang, F.P., Cui, J.J., Chen, X.H., Zhang, S.H., Miao, L.C., Li, J.H., Shi, W., Li, Z.H., Huang, S.Q., and Li, H.L., 2015, Late Jurassic–Early Cretaceous continental convergence and intracontinental orogenesis in East Asia: A synthesis of the Yanshan revolution: Journal of Asian Earth Sciences, v. 114, p. 750–770. doi:10.1016/j.jseaes.2015.08.011

Drummond, M.S., and Defant, M.J., 1990, A model for trondhjemite–tonalite–dacite genesis and crustal growth via slab melting: Archean to modern comparisons: Journal of Geophysical Research, v. 95, p. 21503–21521. doi:10.1029/JB095iB13p21503

Fan, W.M., and Menzies, M.A., 1992, Destruction of aged lower lithosphere and accretion of asthenosphere mantle beneath eastern China: Geotectonica Metallogenia, v. 16, p. 171–180.

Fan, W.M., Zhang, H.F., Baker, J., Jarvis, K.E., Mason, P.R.D., and Menzies, M.A., 2000, On and off the north China craton: Where is the Archaean keel?: Journal of Petrology, v. 41, p. 933–950. doi:10.1093/petrology/41.7.933

Feeley, T.C., and Hacker, M.D., 1995, Intracrustal derivation of Na-rich andesitic and dacitic magmas: An example from Volcán Ollagüe, Andean central volcanic zone: The Journal of Geology, v. 103, p. 213–225. doi:10.1086/629737

Gao, S., Rudnick, R.L., Carlson, R.W., McDonough, W.F., and Liu, Y.S., 2002, Re–Os evidence for replacement of ancient mantle lithosphere beneath the North China craton: Earth and Planetary Science Letters, v. 198, p. 307–322. doi:10.1016/S0012-821X(02)00489-2

Gao, S., Rudnick, R.L., Yuan, H.L., Liu, X.M., Liu, Y.S., Xu, W.L., Ling, W.L., Ayers, J., Wang, X.C., and Wang, Q.H., 2004, Recycling lower continental crust in the North China craton: Nature, v. 432, p. 892–897. doi:10.1038/nature03162

Gao, X.Y., Zhao, T.P., Bao, Z.W., and Yang, A.Y., 2014a, Petrogenesis of the early Cretaceous intermediate and felsic intrusions at the southern margin of the North China Craton: Implications for crust–mantle interaction: Lithos, v. 206–207, p. 65–78. doi:10.1016/j.lithos.2014.07.019

Gao, X.Y., Zhao, T.P., and Chen, W.T., 2014b, Petrogenesis of the early Cretaceous Funiushan granites on the southern margin of the North China Craton: Implications for the Mesozoic geological evolution: Journal of Asian Earth Sciences, v. 94, p. 28–44. doi:10.1016/j.jseaes.2014.07.042

Gao, X.Y., Zhao, T.P., Yuan, Z.L., Zhou, Y.Y., and Gao, J.F., 2010, Geochemistry and petrogenesis of the Heyu batholith in the southern margin of the North China block: Acta Petrologica Sinica, v. 26, p. 3485–3506. (in Chinese with English abstract).

Ge, X.Y., Li, X.H., Chen, Z.G., and Li, W.P., 2002, Geochemistry and petrogenesis of Jurassic high Sr/low Y granitoids in eastern China: Constrains on crustal thickness: Chinese Science Bulletin, v. 47, no. 11, p. 962–968. doi:10.1360/02tb9216

Goldfarb, R.J., and Santosh, M., 2014, The dilemma of the Jiaodong gold deposits: Are they unique?: Geoscience Frontiers, v. 5, p. 139–153. doi:10.1016/j.gsf.2013.11.001

Guo, B., Zhu, L.M., Li, B., Gong, H.J., and Wang, J., 2009, Zircon U–Pb age and Hf isotope composition of the Huashan and Heyu granite plutons at the southern margin of North China Craton: Implication for geodynamic setting: Acta Petrologica Sinica, v. 25, no. 2, p. 265–281. (in Chinese with English abstract).

Guo, P., Santosh, M., and Li, S., 2013, Geodynamics of gold metallogeny in the Shandong Province, NE China: An integrated geological, geophysical and geochemical perspective: Gondwana Research, v. 24, no. 3–4, p. 1172–1202. doi:10.1016/j.gr.2013.02.004

Hacker, B.R., Ratschbacher, L., Webb, L.E., Ireland, T., Walker, D., and Dong, S.W., 1998, U–Pb zircon ages constrain the architecture of the ultrahigh-pressure Qinling–Dabie orogen, China: Earth and Planetary Science Letters, v. 161, p. 215–230. doi:10.1016/S0012-821X(98)00152-6

He, X.X., Tang, S.H., Zhu, X.K., and Wang, J.H., 2007, Precise measurement of Nd isotopic ratios by means of multi-collector magnetic sector inductively coupled plasma mass spectrometry: Acta Geoscientica Sinica, v. 28, no. 4, p. 405–410. [In Chinese with English abstract.]

He, Y.S., Li, S.G., Hoefs, J., Huang, F., Liu, S.A., and Hou, Z.H., 2011, Post-collisional granitoids from the Dabie orogen: New evidence for partial melting of a thickened continental crust: Geochimica et Cosmochimica Acta, v. 75, p. 3815–3838. doi:10.1016/j.gca.2011.04.011

He, Y.S., Li, S.G., Hoefs, J., and Kleinhanns, I.C., 2013, Sr-Nd-Pb isotopic compositions of Early Cretaceous granitoids from the Dabie orogen: Constraints on the recycled lower continental crust: Lithos, v. 156–159, p. 204–217. doi:10.1016/j.lithos.2012.10.011

Hou, M.L., Jiang, Y.H., Jiang, S.Y., Ling, H.F., and Zhao, K.D., 2007, Contrasting origins of late Mesozoic adakitic granitoids from the northwestern Jiaodong Peninsula, east China: Implications for crustal thickening to delamination: Geological Magazine, v. 144, p. 619–631. doi:10.1017/S0016756807003494

Hu, F.Y., Liu, S.W., Santosh, M., Deng, Z.B., Wang, W., Zhang, W. Y., and Yan, M., 2016, Chronology and tectonic implications of Neoproterozoic blocks in the South Qinling Orogenic Belt, Central China: Gondwana Research, v. 30, p. 24–47. doi:10.1016/j.gr.2015.01.006

Hu, G.H., Zhao, T.P., and Zhou, Y.Y., 2014, Depositional age, provenance and tectonic setting of the Proterozoic Ruyang Group, southern margin of the North China Craton: Precambrian Research, v. 246, p. 296–318. doi:10.1016/j.precamres.2014.03.013

Hu, J., Jiang, S.Y., Zhao, H.X., Shao, Y., Zhang, Z.Z., Xiao, E., Wang, Y., Dai, B.Z., and Li, H.Y., 2012, Geochemistry and petrogenesis of the Huashan granites and their implications for the Mesozoic tectonic settings in the Xiaoqinling gold mineralization belt, NW China: Journal of Asian Earth Sciences, v. 56, p. 276–289. doi:10.1016/j.jseaes.2012.05.016

Huang, F., Li, S.G., Dong, F., He, Y.S., and Chen, F.K., 2008, High-Mg adakitic rocks in the Dabie orogen, central China: Implications for foundering mechanism of lower continental crust: Chemical Geology, v. 255, p. 1–13. doi:10.1016/j.chemgeo.2008.02.014

Huang, X., and Wu, L.R., 1990, Nd–Sr isotopes of granitoids from Shanxi Province and their significance for tectonic evolution: Acta Petrologica Sinica, v. 6, p. 1–11. [In Chinese with English abstract.]

Jackson, S.E., Pearson, N.J., Griffin, W.L., and Belousova, E.A., 2004, The application of laser ablation–inductively coupled plasma–mass spectrometry to in situ U–Pb zircon geochronology: Chemical Geology, v. 211, p. 47–69. doi:10.1016/j.chemgeo.2004.06.017

Jiang, N., Liu, Y.S., Zhou, W.G., Yang, J.H., and Zhang, S.Q., 2007, Derivation of Mesozoic adakitic magmas from ancient lower crust in the North China craton: Geochimica et Cosmochimica Acta, v. 71, p. 2591–2608. doi:10.1016/j.gca.2007.02.018

Kröner, A., Compston, W., Zhang, G.W., Guo, A., and Todt, W., 1988, Age and tectonic setting of Late Archean greenstone–gneiss terrain in Henan province, China, as revealed by single grain zircon dating: Geology, v. 16, p. 211–215. doi:10.1130/0091-7613(1988)016<0211:AATSOL>2.3.CO;2

Li, H.K., Geng, J.Z., Hao, S., Zhang, Y.Q., and Li, H.M., 2009, Studies on measuring the U–Pb isotopic age of zircon by using laser ablation multi-collector inductively coupled plasma mass spectrometry (LA–MC–ICP MS): Acta Mineralogica Sinica, v. S1, p. 600–601. (in Chinese with English abstract).

Li, J.H., Zhang, Y.Q., Dong, S.W., and Shi, W., 2013a, Structural and geochronological constraints on the Mesozoic tectonic evolution of the North Dabashan zone, South Qinling, central China: Journal of Asian Earth Sciences, v. 64, p. 99–114. doi:10.1016/j.jseaes.2012.12.001

Li, L., Sun, W.Z., Meng, X.F., Zhang, D.T., Yang, X.F., and Feng, J. Z., 2013b, Geochemical and Sr–Nd–Pb isotopic characteristics of the granitoids of Xiaoshan Mountain area on the southern margin of North China Block and its geological significance: Acta Petrologica Sinica, v. 29, no. 8, p. 2635–2652. (in Chinese with English abstract).

Li, N., Chen, Y.J., Pirajno, F., Gong, H.J., Mao, S.D., and Ni, Z.Y., 2012, LA-ICP-MS zircon U–Pb dating, trace element and Hf isotope geochemistry of the Heyu granite batholith, eastern Qinling, central China: Implications for Mesozoic tectono-magmatic evolution: Lithos, v. 142–143, p. 34–47. doi:10.1016/j.lithos.2012.02.013

Li, S.G., Xiao, Y.L., Liou, D.L., Chen, Y.Z., Ge, N.J., Zhang, Z.Q., Sun, S.S., Cong, B.L., Zhang, R.Y., Hart, S.R., and Wang, S.S., 1993, Collision of the North China and Yangtse blocks and formation of coesite-bearing eclogites: Timing and processes: Chemical Geology, v. 109, p. 89–111. doi:10.1016/0009-2541(93)90063-O

Litvinovsky, B.A., Steele, I.M., and Wickham, S.M., 2000, Silicic magma formation in overthickened crust: Melting of charnockite and leucogranite at 15, 20 and 25 kbar: Journal of Petrology, v. 41, no. 5, p. 717–737. doi:10.1093/petrology/41.5.717

Liu, S.A., Li, S.G., Guo, S.S., Hou, Z.H., and He, Y.S., 2012, The Cretaceous adakitic–basaltic–granitic magma sequence on south-eastern margin of the North China Craton: Implications for lithospheric thinning mechanism: Lithos, v. 134–135, p. 163–178. doi:10.1016/j.lithos.2011.12.015

Liu, S.W., Zhang, J.J., and Zheng, Y.D., 1998, Syn-deformation P-T paths of Xiaoqinling metamorphic core complex: Chinese Science Bulletin, v. 43, p. 1927–1934. doi:10.1007/BF02883474

Liu, X.C., Jahn, B.M., Cui, J.J., Li, S.Z., Wu, Y.B., and Li, X.H., 2010a, Triassic retrograded eclogites and Cretaceous gneissic granites in the Tongbai Complex, central China: Implications for the architecture of the HP/UHP Tongbai–Dabie–Sulu collision zone: Lithos, v. 119, p. 211–237. doi:10.1016/j.lithos.2010.06.005

Liu, X.C., Jahn, B.M., Hu, J., Li, S.Z., Liu, X., and Song, B., 2011, Metamorphic patterns and SHRIMP zircon ages of medium–to–high grade rocks from the Tongbai orogen, central China: Implications for multiple accretion/collision processes prior to terminal continental collision: Journal of Metamorphic Geology, v. 29, p. 979–1002. doi:10.1111/j.1525-1314.2011.00952.x

Liu, X.C., Jahn, B.M., Li, S.Z., and Liu, Y.S., 2013, U–Pb Zircon age and geochemical constraints on tectonic evolution of the Paleozoic accretionary orogenic system in the Tongbai orogen, central China: Tectonophysics, v. 29, p. 233–249.

Liu, Y.S., Gao, S., Hu, Z.C., Gao, C.G., Zong, K.Q., and Wang, D.B., 2010b, Continental and oceanic crust recycling-induced melt–peridotite interactions in the Trans-North China orogen: U–Pb dating, Hf isotopes and trace elements in zircons from mantle xenoliths: Journal of Petrology, v. 51, p. 537–571. doi:10.1093/petrology/egp082

Liu, Y.S., Gao, S., Yuan, H.L., Zhou, L., Liu, X.M., Wang, X.C., Hu, Z.C., and Wang, L.S., 2004, U–Pb zircon ages and Nd, Sr, and Pb isotopes of lower crustal xenoliths from North China Craton: Insights on evolution of lower continental crust: Chemical Geology, v. 211, p. 87–109. doi:10.1016/j.chemgeo.2004.06.023

Liu, Y.S., Hu, Z.C., Gao, S., Gunther, D., Xu, J., Gao, C.G., and Chen, H.H., 2008, In situ analysis of major and trace elements of anhydrous minerals by LA–ICP–MS without applying an internal standard: Chemical Geology, v. 257, p. 34–43. doi:10.1016/j.chemgeo.2008.08.004

Lu, S.N., Zhao, G.C., Wang, H.C., and Hao, G.J., 2008, Precambrian metamorphic basement and sedimentary cover of the North China Craton: A review: Precambrian Research, v. 160, p. 77–93. doi:10.1016/j.precamres.2007.04.017

Ludwig, K.R., 2003, User's manual for Isoplot 3.00. A geochronological toolkit for Microsoft Excel: Berkeley Geochronology Center. Special Publication, No. 4a. doi: bgc.org/isoplot_etc/isoplot/Isoplot3_75-4_15manual.pdf

Macpherson, C.G., Dreher, S., and Thirlwall, M.F., 2006, Adakites without slab melting: High pressure differentiation of island arc magma, Mindanao, the Philippines: Earth and Planetary Science Letters, v. 243, p. 581–593. doi:10.1016/j.epsl.2005.12.034

Mao, J.W., Goldfarb, R., Zhang, Z.W., Xu, W.Y., Qiu, Y.M., and Deng, J., 2002, Gold deposits in the Xiaoqinling-Xiong'ershan region, Qinling Mountains, central China: Mineralium Deposita, v. 37, no. 3–4, p. 306–325. doi:10.1007/s00126-001-0248-1

Mao, J.W., Pirajno, F., Xiang, J.F., Gao, J.J., Ye, H.S., Li, Y.F., and Guo, B.J., 2011, Mesozoic molybdenum deposits in the east Qinling-Dabie orogenic belt: Characteristics and tectonic settings: Ore Geology Reviews, v. 43, p. 264–293. doi:10.1016/j.oregeorev.2011.07.009

Mao, J.W., Xie, G.Q., Pirajno, F., Ye, H.S., Wang, Y.B., Li, Y.F., Xiang, J.F., and Zhao, H.J., 2010, Late Jurassic-early Cretaceous granitoid magmatism in East Qinling, central eastern China: SHRIMP zircon U–Pb ages and tectonic implications: Australian Journal of Earth Sciences, v. 57, p. 51–78. doi:10.1080/08120090903416203

Mao, J.W., Xie, G.Q., Zhang, Z.H., Li, X.F., Wang, Y.T., Zhang, C. Q., and Li, Y.F., 2005, Mesozoic large-scale metallogenic pulses in North China and corresponding geodynamic settings: Acta Petrologica Sinica, v. 21, no. 1, p. 169–188.

Martin, H., 1999, Adakitic magmas: Modern analogues of Archaean granitoids: Lithos, v. 46, p. 411–429. doi:10.1016/S0024-4937(98)00076-0

Menzies, M., Xu, Y.G., Zhang, H.F., and Fan, W.M., 2007, Integration of geology, geophysics and geochemistry: A key to understanding the North China Craton: Lithos, v. 96, p. 1–21. doi:10.1016/j.lithos.2006.09.008

Menzies, M.A., Fan, W., and Zhang, M., 1993, Palaeozoic and Cenozoic lithoprobes and the loss of N120 km of Archaean lithosphere, Sino-Korean craton, China: Geological Society, London, Special Publications, v. 76, no. 1, p. 71–81. doi:10.1144/GSL.SP.1993.076.01.04

Middlemost, E.A.K., 1994, Naming materials in the magma/igneous rock system: Earth Science Reviews, v. 37, p. 215–224. doi:10.1016/0012-8252(94)90029-9

Nash, W.P., and Crecraft, H.R., 1985, Partition coefficients for trace elements in silicic magmas: Geochimica et Cosmochimica Acta, v. 49, p. 2309–2322. doi:10.1016/0016-7037(85)90231-5

Ni, Z.Y., Li, N., Zhang, H., and Xue, L.W., 2009, Pb–Sr–Nd isotopic constrains on the source of ore-forming elements of the Dahu Au–Mo deposit, Henan province: Acta Petrologica Sinica, v. 25, p. 2823–2832. [In Chinese with English abstract.]

Otamendi, J.E., De La Rosa, J.D., Patiño Douce, A.E., and Castro, A., 2002, Rayleigh fractionation of heavy rare earths and yttrium during metamorphic garnet growth: Geology, v. 30, no. 2, p. 159–162. doi:10.1130/0091-7613(2002)030<0159:RFOHRE>2.0.CO;2

Patiño Douce, A.E., 2005, Vapor-absent melting of tonalite at 15–32 kbar: Journal of Petrology, v. 46, no. 2, p. 275–290. doi:10.1093/petrology/egh071

Petford, N., and Atherton, M., 1996, Na-rich partial melts from newly underplated basaltic crust: The Cordillera Blanca Batholith, Peru: Journal of Petrology, v. 37, p. 1491–1521. doi:10.1093/petrology/37.6.1491

Ping, X.Q., Zheng, J.P., Tang, H.Y., Xiong, Q., and Su, Y.P., 2015, Paleoproterozoic multistage evolution of the lower

crust beneath thesouthern North China Craton: Precambrian Research, v. 269, p. 162–182. doi:10.1016/j.precamres.2015.08.001
Qi, Q.J., Wang, X.X., Ke, C.H., and Li, J.B., 2012, Geochronology and origin of the Laoniushan complex in the southern margin of North China Block and their implications: New evidences from zircon dating, Hf isotopes and geochemistry: Acta Petrologica Sinica, v. 28, no. 1, p. 279–301. (in Chinese with English abstract).
Qin, J.F., Lai, S.C., Grapes, R., Diwu, C., Ju, Y.J., and Li, Y.F., 2009, Geochemical evidence for origin of magma mixing for the Triassic monzonitic granite and its enclaves at Mishuling in the Qinling orogen (central China): Lithos, v. 112, p. 259–276. doi:10.1016/j.lithos.2009.03.007
Rapp, R.P., 1995, Amphibole-out phase boundary in partially melted metabasalt, its control over liquid fraction and composition, and source permeability: Journal of Geophysical Research, v. 100, p. 15601–15610. doi:10.1029/95JB00913
Rapp, R.P., and Watson, E.B., 1995, Dehydration melting of metabasalt at 8–32 kbar: Implications for continental growth and crust-mantle recycling: Journal of Petrology, v. 36, p. 891–931. doi:10.1093/petrology/36.4.891
Rapp, R.P., Watson, E.B., and Miller, C.F., 1991, Partial melting of amphibolite/eclogite and the origin of Archean trondhjemites and tonalities: Precambrian Research, v. 51, p. 1–25. doi:10.1016/0301-9268(91)90092-O
Rudnick, R., and Gao, S., 2003, Composition of the continental crust, *in* Holland, H.D., and Turekian, K.K., eds., Treatise on geochemistry: Amsterdam, Elsevier, p. 1–64.
Rudnick, R.L., and Fountain, D.M., 1995, Nature and composition of the continental crust: A lower crustal perspective: Reviews of Geophysics, v. 33, p. 267–309. doi:10.1029/95RG01302
Rudnick, R.L., Gao, S., Ling, W.L., Liu, Y.S., and McDonough, W. F., 2004, Petrology and geochemistry of spinel peridotite xenoliths from Hannuoba and Qixia, North China Craton: Lithos, v. 77, p. 609–637. doi:10.1016/j.lithos.2004.03.033
Santosh, M., 2010, Assembling North China Craton within the Columbia supercontinent: The role of double-sided subduction: Precambrian Research, v. 178, p. 149–167. doi:10.1016/j.precamres.2010.02.003
Santosh, M., Wilde, S.A., and Li, J.H., 2007, Timing of Paleoproterozoic ultrahigh temperature metamorphism in the North China Craton: Evidence from SHRIMP U–Pb zircon geochronology: Precambrian Research, v. 159, p. 178–196. doi:10.1016/j.precamres.2007.06.006
Sen, C., and Dunn, T., 1994, Dehydration melting of a basaltic composition amphibolite at 1.5 and 2.0 GPa: Implications for the origin of adakites: Contributions to Mineralogy and Petrology, v. 117, p. 394–409. doi:10.1007/BF00307273
Smithies, R.H., and Champion, D.C., 2000, The Archean high-Mg diorite suite: Links to tonalite–trondhjemite–granodiorite magmatism and implications for early Archean crustal growth: Journal of Petrology, v. 41, p. 1653–1671. doi:10.1093/petrology/41.12.1653
Springer, W., and Seck, H.A., 1997, Partial fusion of basic granulite at 5 to 15 kbar: Implications for the origin of TTG magmas: Contrib. Contributions to Mineralogy and Petrology, v. 127, p. 30–45. doi:10.1007/s004100050263
Streckeisen, A., 1976, To each plutonic rock its proper name: Earth-Science Reviews, v. 12, p. 1–33. doi:10.1016/0012-8252(76)90052-0
Sun, S.S., and Mcdonough, W.F., 1989, Chemical and isotopic systematics of oceanic basalts: Implications for mantle composition and processes, *in* Sanuder, A.D., and Norry, M.J., eds., Magmatism in the Ocean Basins, Volume 42: Geological Society Special Publication, 313–345 p.
Tang, H.Y., Zheng, J.P., Griffin, W.L., O'Reilly, S.Y., Yu, C.M., Pearson, N., Ping, X.Q., Xia, B., and Yang, H.B., 2014, Complex evolution of the lower crust beneath the southeastern North China Craton: The Junan xenoliths and xenocrysts: Lithos, v. 206–207, p. 113–126. doi:10.1016/j.lithos.2014.07.018
Tang, Y.J., Zhang, H.F., Santosh, M., and Ying, J.F., 2013, Differential destruction of the North China Craton: A tectonic perspective: Journal of Asian Earth Sciences, v. 78, p. 71–82. doi:10.1016/j.jseaes.2012.11.047
Wan, Y.S., Wilde, S.A., Liu, D.Y., Yang, C.X., Song, B., and Yin, X. Y., 2006, Further evidence for 1.85 Ga metamorphism in the Central Zone of the North China Craton: SHRIMP U–Pb dating of zircon from metamorphic rocks in the Lushan area, Henan Province: Gondwana Research, v. 9, p. 189–197. doi:10.1016/j.gr.2005.06.010
Wang, L., He, H.L., and Li, B., 2003, Multi-element determination in geological samples by inductively coupled plasma mass spectrometry after fusion-precipitation treatment: Rocks and Mineral Analysis, v. 22, p. 86–92. (in Chinese with English abstract)
Wang, Q., Wyman, D.A., Xu, J.F., Jian, P., Zhao, Z.H., Li, C.H., Xu, W., Ma, J.L., and He, B., 2007a, Early Cretaceous adakitic granites in the Northern Dabie Complex, central China: Implications for partial melting and delamination of thickened lower crust: Geochimica et Cosmochimica Acta, v. 71, p. 2609–2636. doi:10.1016/j.gca.2007.03.008
Wang, Q., Xu, J.F., Jian, P., Bao, Z.W., Zhao, Z.H., Li, C.F., Xiong, X.L., and Ma, J.L., 2006, Petrogenesis of adakitic porphyries in an extensional tectonic setting, Dexing, South China: Implications for the genesis of porphyry copper mineralization: Journal of Petrology, v. 47, p. 119–144. doi:10.1093/petrology/egi070
Wang, X.X., Wang, T., Castro, A., Pedreira, R., Lu, X.X., and Xiao, Q.H., 2011, Triassic granitoids of the Qinling orogen, central China: Genetic relationship of enclaves and rapakivi-textured rocks: Lithos, v. 126, p. 369–387. doi:10.1016/j.lithos.2011.07.007
Wang, X.X., Wang, T., Happala, I., and Lu, X.X., 2005, Genesis of mafic enclaves from rapakivi-textured granites in the Qinling and its petrological significance: Evidence of elements and Nd, Sr isotopes: Acta Petrologica Sinica, v. 20, p. 935–946. (in Chinese with English abstract)
Wang, X.X., Wang, T., Jahn, B.M., Hu, N.G., and Chen, W., 2007b, Tectonic significance of Late Triassic post-collisional lamprophyre dykes from the Qinling Mountains (China): 40Ar–39Ar dating, trace element and Sr–Nd, isotope characteristics: Geological Magazine, v. 144, no. 4, p. 1–12. doi:10.1017/S0016756807003548
Wang, X.X., Wang, T., and Zhang, C.L., 2013, Neoproterozoic, Paleozoic, and Mesozoic granitoid magmatism in the Qinling Orogen, China: Constraints on orogenic process: Journal of Asian Earth Sciences, v. 72, p. 129–151. doi:10.1016/j.jseaes.2012.11.037
Wareham, C.D., Millar, I.L., and Vaughan, A.P.M., 1997, The generation of sodic granite magmas, western Palmer Land, Antarctic Peninsula: Contributions to Mineralogy

and Petrology, v. 128, p. 81–96. doi:10.1007/s004100050295
Wu, F.Y., Lin, J.Q., Wilde, S.A., Zhang, X.O., and Yang, J.H., 2005, Nature and significance of the early Cretaceous giant igneous event in eastern China: Earth and Planetary Science Letters, v. 233, p. 103–119. doi:10.1016/j.epsl.2005.02.019
Wu, Y.B., and Zheng, Y.F., 2013, Tectonic evolution of a composite collision orogen: An overview on the Qinling–Tongbai–Hong'an–Dabie–Sulu orogenic belt in central China: Gondwana Research, v. 23, p. 1402–1428. doi:10.1016/j.gr.2012.09.007
Xu, H.J., Ma, C.Q., and Ye, K., 2007, Early cretaceous granitoids and their implications for the collapse of the Dabie orogen, eastern China: SHRIMP zircon U–Pb dating and geochemistry: Chemical Geology, v. 240, p. 238–259. doi:10.1016/j.chemgeo.2007.02.018
Xu, H.J., Ma, C.Q., Zhang, J.F., and Ye, K., 2012, Early Cretaceous low-Mg adakitic granites from the Dabie orogen, eastern China: Petrogenesis and implications for destruction of the over-thickened lower continental crust: Gondwana Research, v. 23, no. 1, p. 190–207. doi:10.1016/j.gr.2011.12.009
Xu, J.F., Shinjio, R., Defant, M.J., Wang, Q., and Rapp, R.P., 2002, Origin of Mesozoic adakitic intrusive rocks in the Ningzhen area of east China: Partial melting of delaminated lower continental crust?: Geology, v. 12, p. 1111–1114. doi:10.1130/0091-7613(2002)030<1111:OOMAIR>2.0.CO;2
Xu, W.L., Hergt, J.H., Gao, S., Pei, F.P., Wang, W., and Yang, D.B., 2008, Interaction of adakitic melt-peridotite: Implications for the high-Mg# signature of Mesozoic adakitic rocks in the eastern North China Craton: Earth and Planetary Science Letters, v. 265, p. 123–137. doi:10.1016/j.epsl.2007.09.041
Xu, W.L., Pei, F.P., Wang, F., Meng, E., Ji, W.Q., Yang, D.B., and Wang, W., 2013, Spatial–temporal relationships of Mesozoic volcanic rocks in NE China: Constraints on tectonic overprinting and transformations between multiple tectonic systems: Journal of Asian Earth Sciences, v. 74, p. 167–193. doi:10.1016/j.jseaes.2013.04.003
Xu, W.L., Wang, Q.H., Wang, D.Y., Guo, J.H., and Pei, F.P., 2006, Mesozoic adakitic rocks from the Xuzhou–Suzhou area, eastern China: Evidence for partial melting of delaminated lower continental crust: Journal of Asian Earth Sciences, v. 27, p. 454–464. doi:10.1016/j.jseaes.2005.03.010
Xu, X.S., Griffin, W.L., Ma, X., O'Reilly, S.Y., He, Z.Y., and Zhang, C.L., 2009, The Taihua group on the southern margin of the North China craton: Further insights from U–Pb ages and Hf isotope compositions of zircons: Mineralogy and Petrology, v. 97, p. 43–59. doi:10.1007/s00710-009-0062-5
Xu, Y.G., 2001, Thermo-tectonic destruction of the Archean lithospheric keel beneath the Sino-Korean craton in China: Evidence, timing and mechanism: Physics and Chemistry of the Earth, v. Part A 26, p. 747–757. doi:10.1016/S1464-1895(01)00124-7
Xu, Y.G., Huang, X.L., Ma, J.L., Wang, Y.B., Iizuka, Y., Xu, J.F., Wang, Q., and Wu, X.Y., 2004, Crust-mantle interaction during the tectono-thermal reactivation of the North China Craton: Constraints from SHRIMP zircon U–Pb chronology and geochemistry of Mesozoic plutons from western Shandong: Contributions to Mineralogy and Petrology, v. 147, p. 750–767. doi:10.1007/s00410-004-0594-y
Xue, F., Lerch, M.F., Kröner, A., and Reischmann, T., 1996, Tectonic evolution of the East Qinling Mountains, China, in the Palaeozoic: A review and new tectonic model: Tectonophysics, v. 253, p. 271–284. doi:10.1016/0040-1951(95)00060-7
Xue, L.W., Yuan, Z.L., and Zhang, Y.S., 1995, The Sm–Nd isotope age of Taihua group in Lushan area and their implications: Geochimica, v. 24, p. 92–97. (in Chinese with English abstract).
Yang, D.B., Xu, W.L., Wang, Q.H., and Pei, F.P., 2010, Chronology and geochemistry of Mesozoic granitoids in the Bengbu area, central China: Constraints on the tectonic evolution of the eastern North China Craton: Lithos, v. 114, no. 1–2, p. 200–216. doi:10.1016/j.lithos.2009.08.009
Yang, D.B., Xu, W.L., Zhao, G.C., Huo, T.F., Shi, J.P., and Yang, H. T., 2016, Tectonic implications of Early Cretaceous low-Mg adakitic rocks generated by partial melting of thickened lower continental crust at the southern margin of the central North China Craton: Gondwana Research, v. 38, p. 220–237. doi:10.1016/j.gr.2015.11.013
Yang, J.H., Wu, F.Y., Chung, S.L., Wilde, S.A., Chu, M.F., Lo, C.H., and Song, B., 2005, Petrogenesis of Early Cretaceous intrusions in the Sulu ultrahigh-pressure orogenic belt, east China and their relationship to lithospheric thinning: Chemical Geology, v. 222, p. 200–231. doi:10.1016/j.chemgeo.2005.07.006
Yogodzinski, G.M., Lees, J.M., Churikova, T.G., Dorendorf, F., Woerner, G., and Volynets, O.N., 2001, Geochemical evidence for the melting of subducting oceanic lithosphere at plate edges: Nature, v. 409, p. 500–504. doi:10.1038/35054039
Yu, S.Y., Zhang, J.X., Qin, H.P., Sun, D.Y., Zhao, X.L., Cong, F., and Li, Y.D., 2015, Petrogenesis of the early Paleozoic low-Mg and high-Mg adakitic rocks in the North Qilian orogenic belt, NW China: Implications for transition from crustal thickening to extension thinning: Journal of Asian Earth Sciences, v. 107, p. 122–139. doi:10.1016/j.jseaes.2015.04.018
Zhang, C., Ma, C.Q., and Holtz, F., 2010, Origin of high-Mg adakitic magmatic enclaves from the Meichuan pluton, southern Dabie orogen (central China): Implications for delamination of the lower continental crust and melt-mantle interaction: Lithos, v. 119, p. 467–484. doi:10.1016/j.lithos.2010.08.001
Zhang, G.W., Zhang, B.R., Yuan, X.C., and Xiao, Q.H., 2001, Qinling orogenic belt and continental dynamics: Beijing, Science Press, 1–855 p.
Zhang, H.F., Gao, S., Zhong, Z.Q., Zhang, B.R., Zhang, L., and Hu, S.H., 2002, Geochemical and Sr–Nd–Pb isotopic compositions of Cretaceous granitoids: Constrains on tectonic framework and crustal structure of the Dabieshan ultrahigh-pressure metamorphic belt, China: Chemical Geology, v. 186, p. 281–299. doi:10.1016/S0009-2541(02)00006-2
Zhang, H.F., Ge, L.L., Zhang, L., Harris, N., Zhou, L., Hu, S.H., and Zhang, B.R., 2005, Geochemistry and Pb–Sr–Nd composition of the granitoids in the West Qinling: Constrain to the basement and tectonics: Science in China (Series D), v. 35, no. 10, p. 914–926.
Zhang, H.F., Yang, Y.H., Santosh, M., Zhao, X.M., Ying, J.F., and Xiao, Y., 2012, Evolution of the Archean and Paleoproterozoic lower crust beneath the Trans-North China Orogen and the Western Block of the North China Craton: Gondwana Research, v. 22, p. 73–85. doi:10.1016/j.gr.2011.08.011

Zhang, H.F., Zhu, R.X., Santosh, M., Ying, J.F., Su, B.X., and Hu, Y., 2013, Episodic widespread magma underplating beneath the North China Craton in the Phanerozoic: Implications for craton destruction: Gondwana Research, v. 23, no. 1, p. 95–107. doi:10.1016/j.gr.2011.12.006

Zhang, J.J., and Zheng, Y.D., 1999, The multiphase extension and their ages of the Xiaoqinling metamorphic core complex: Acta Geologica Sinica, v. 73, no. 2, p. 139–147. doi:10.1111/j.1755-6724.1999.tb00821.x

Zhang, Y.Q., Dong, S.W., Zhao, Y., and Zhang, T., 2007, Jurassic tectonics of North China: A Synthetic view: Acta Geologica Sinica, v. 11, p. 1462–1480. (in Chinese with English abstract)

Zhao, G.C., Cawood, P.A., Li, S.Z., Wilde, S.A., Sun, M., Zhang, J., He, Y.H., and Yin, C.Q., 2012b, Amalgamation of the North China Craton: Key issues and discussion: Precambrian Research, v. 222–223, p. 55–76. doi:10.1016/j.precamres.2012.09.016

Zhao, G.C., He, Y.H., and Sun, M., 2009, The Xiong'er volcanic belt at the southern mar-gin of the North China Craton: Petrographic and geochemical evidence for its outboard position in the Paleo-Mesoproterozoic Columbia Supercontinent: Gondwana Research, v. 16, no. 2, p. 170–181. doi:10.1016/j.gr.2009.02.004

Zhao, G.C., Peter, A., Cawood, P.A., Wilde, S.A., Sun, M., and Lu, L. Z., 2000, Metamorphism of basement rocks in the Central Zone of the North China Craton: Implications for Paleoproterozoic tectonic evolution: Precambrian Research, v. 103, p. 55–88. doi:10.1016/S0301-9268(00)00076-0

Zhao, G.C., Sun, M., Wilde, S.A., and Li, S.Z., 2005a, Late Archean to Paleoproterozoic evolution of the North China Craton: Key issues revisited: Precambrian Research, v. 136, p. 177–202. doi:10.1016/j.precamres.2004.10.002

Zhao, G.C., Wilde, S.A., Sun, M., Li, S.Z., Li, X.P., and Zhang, J., 2008, SHRIMP U–Pb zircon ages of granitoid rocks in the Lüliang Complex: Implications for the accretion and evolution of the Trans-North China Orogen: Precambrian Research, v. 160, p. 213–226. doi:10.1016/j.precamres.2007.07.004

Zhao, H.X., Jiang, S.Y., Frimmel, H.E., Dai, B.Z., and Ma, L., 2012a, Geochemistry, geochronology and Sr–Nd–Hf isotopes of two Mesozoic granitoids in the Xiaoqinling gold district: Implication for large-scale lithospheric thinning in the North China Craton: Chemical Geology, v. 294–295, p. 173–189. doi:10.1016/j.chemgeo.2011.11.030

Zhao, J.H., and Zhou, M.F., 2007, Neoproterozoic adakitic plutons and arc magmatism along the western margin of the Yangtze Block, South China: Journal of Geology, v. 115, p. 675–689. doi:10.1086/521610

Zhao, T.P., Zhai, M.G., Xia, B., Li, H.M., Zhang, Y.X., and Wan, Y. S., 2004, Zircon U–Pb SHRIMP dating for the volcanic rocks of the Xiong'er Group: Constraints on the initial formation age of the cover of the North China Craton: China Science Bulletin, v. 49, no. 23, p. 2495–2502. doi:10.1007/BF03183721

Zhao, Z.F., Zheng, Y.F., Wei, C.S., and Wu, Y.B., 2007, Post-collisional granitoids from the Dabie orogen in China: Zircon U–Pb age, element and O isotope evidence for recycling of subducted continental crust: Lithos, v. 93, p. 248–272. doi:10.1016/j.lithos.2006.03.067

Zhao, Z.F., Zheng, Y.F., Wei, C.S., Wu, Y.B., Chen, F.K., and Jahn, B.M., 2005b, Zircon U–Pb age, element and C–O isotope geochemistryof post-collisional mafic–ultramafic rocks from the Dabie orogen in east-central China: Lithos, v. 83, p. 1–28. doi:10.1016/j.lithos.2004.12.014

Zheng, J.P., Griffin, W.L., O'Reilly, S.Y., Hu, B.Q., Zhang, M., Pearson, N., Wang, F.Z., and Lu, F.X., 2008, Continental collision/accretion and modification recorded in the deep lithosphere of central China: Earth and Planetary Science Letters, v. 269, p. 496–506. doi:10.1016/j.epsl.2008.03.003

Zheng, J.P., Griffin, W.L., O'Reilly, S.Y., and Lu, F.X., 2004a, 3.6 Ga lower crust in central China: New evidence on the assembly of the North China Craton: Geology, v. 32, p. 229–232. doi:10.1130/G20133.1

Zheng, J.P., Griffin, W.L., O'Reilly, S.Y., Lu, F.X., and Yu, C.M., 2004b, U–Pb and Hf-isotope analysis of zircons in mafic xenoliths from Fuxian kimberlites: Evolution ofthe lower crust beneath the North China Craton: Contributions to Mineralogy and Petrology, v. 148, p. 79–103. doi:10.1007/s00410-004-0587-x

Zheng, J.P., Griffin, W.L., O'Reilly, S.Y., Zhang, M., and Pearson, N., 2006, Zircons in mantle xenoliths record the Triassic Yangtze-North China continental collision: Earth and Planetary Science Letters, v. 247, p. 130–142. doi:10.1016/j.epsl.2006.05.011

Zheng, J.P., O'Reilly, S.Y., Griffin, W.L., Lu, F.X., and Zhang, M., 1998, Nature and evolution of Cenozoic lithospheric mantle beneath Shandong Peninsula, North China Platform: International Geology Review, v. 40, p. 471–499. doi:10.1080/00206819809465220

Zheng, J.P., Sun, M., Lu, F.X., and Pearson, N., 2003, Mesozoic lower crustal xenoliths and their significance in lithospheric evolution beneath the Sino-Korean Craton: Tectonophysics, v. 361, p. 37–60. doi:10.1016/S0040-1951(02)00537-1

Zheng, Y.F., Wang, Z.R., Li, S.G., and Zao, Z.F., 2002, Oxygen isotope equilibrium between eclogite minerals and its constraints on mineral Sm–Nd chronometer: Geochimica et Cosmochimica Acta, v. 66, p. 625–634. doi:10.1016/S0016-7037(01)00801-8

Zhou, X.H., Sun, M., Zhang, G.H., and Chen, S.H., 2002, Continental crust and lithospheric mantle interaction beneath North China: Isotopic evidence from granulite xenoliths in Hannuoba, Sino-Korean craton: Lithos, v. 62, p. 111–124. doi:10.1016/S0024-4937(02)00110-X

Zhu, L.M., Zhang, G.W., Guo, B., and Li, B., 2008, U–Pb (LA–ICP–MS) zircon dating for the large Jinduicheng porphyry Mo deposit in the East China, and its metallogenic setting: Acta Geologica Sinica, v. 82, p. 204–220. (in Chinese with English abstract)